

Journal Pre-proofs

Chemoenzymatic synthesis of enantiomerically enriched diprophylline and xanthinol nicotinate

Paweł Borowiecki, Mateusz Młynek, Maciej Dranka

PII: S0045-2068(20)31746-6
DOI: <https://doi.org/10.1016/j.bioorg.2020.104448>
Reference: YBIOO 104448

To appear in: *Bioorganic Chemistry*

Received Date: 9 August 2020
Revised Date: 28 October 2020
Accepted Date: 29 October 2020

Please cite this article as: P. Borowiecki, M. Młynek, M. Dranka, Chemoenzymatic synthesis of enantiomerically enriched diprophylline and xanthinol nicotinate, *Bioorganic Chemistry* (2020), doi: <https://doi.org/10.1016/j.bioorg.2020.104448>

This is a PDF file of an article that has undergone enhancements after acceptance, such as the addition of a cover page and metadata, and formatting for readability, but it is not yet the definitive version of record. This version will undergo additional copyediting, typesetting and review before it is published in its final form, but we are providing this version to give early visibility of the article. Please note that, during the production process, errors may be discovered which could affect the content, and all legal disclaimers that apply to the journal pertain.

© 2020 Published by Elsevier Inc.



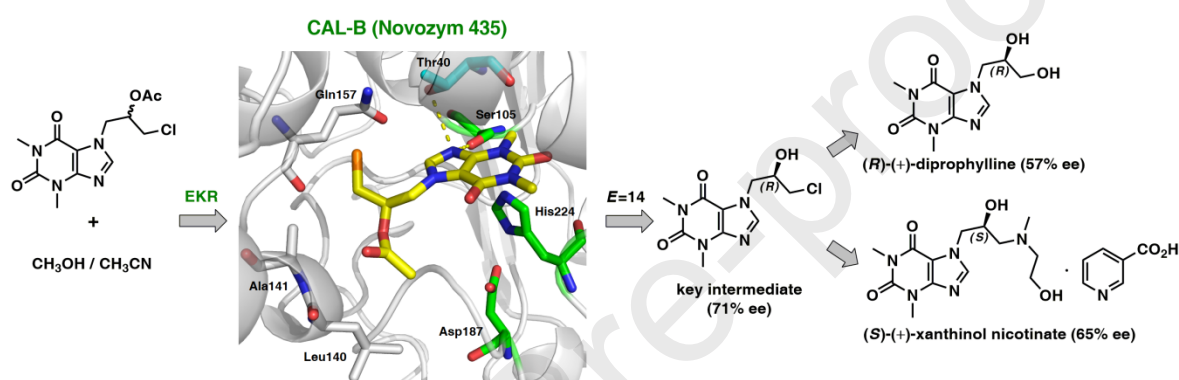
Chemoenzymatic synthesis of enantiomerically enriched diprophylline and xanthinol nicotinate

Paweł Borowiecki,^{*a} Mateusz Młynek,^a and Maciej Dranka^b

^a Warsaw University of Technology, Department of Drugs Technology and Biotechnology, Laboratory of Biocatalysis and Biotransformations, Koszykowa St. 75, 00-662 Warsaw, Poland.

^b Warsaw University of Technology, Faculty of Chemistry, Department of Inorganic Chemistry and Solid State Technology, Noakowskiego 3, 00-664 Warsaw, Poland.

*Corresponding author. E-mail addresses: pawel_borowiecki@onet.eu or pborowiecki@ch.pw.edu.pl.



ABSTRACT: A concise chemoenzymatic route toward enantiomerically enriched active pharmaceutical ingredients (API) – diprophylline and xanthinol nicotinate – is reported for the first time. The decisive step is an enantioselective lipase-mediated methanolysis of racemic chlorohydrin-synthon acetate, namely 1-chloro-3-(1,3-dimethyl-2,6-dioxo-1,2,3,6-tetrahydro-7H-purin-7-yl)propan-2-yl acetate, performed under kinetically-controlled conditions on a preparative 500 mg-scale. The best results in terms of reaction enantioselectivity ($E=14$) were obtained for the enantiomers resolution performed with lipase type B from *Candida antarctica* immobilized on acrylic resin (CAL-B, Novozym 435) suspended in homophasic acetonitrile-methanol mixture. The elaborated biocatalytic system furnished the key chlorohydrin intermediate (in 71% ee and 38% yield), which was then smoothly converted into enantioenriched active agents: (R)-(-)-diprophylline (57% ee) and (S)-(+)-xanthinol nicotinate (65% ee). To support the assignment of absolute configurations of EKR-products as well as to confirm the stereochemical outcome of the remaining reaction steps, docking studies toward the prediction of enantiomers binding selectivity in CAL-B active site as well as the respective chemical correlations with enantiomerically enriched analytical standards obtained from commercially available (R)-(-)-epichlorohydrin, were applied. In addition, single-crystal X-ray diffraction (XRD) analyses were performed for the synthesized optically active APIs furnishing by this manner a first crystal structures of nicotinic acid salt of xanthinol.

Keywords: Enantiomeric APIs, Biocatalysis, Lipases, Kinetic Resolution, Docking Studies.

1. INTRODUCTION

The xanthine ring system is the pervasive structural motif of many natural products and their metabolites exhibiting central nervous system (CNS) stimulant activity. The prominent examples among this group of compounds are plant alkaloids, such as: caffeine, theobromine, theophylline, 7-methylxanthine, paraxanthine, theacrine, 1,3,7-trimethyluric acid, uric acid, methylxanthine, liberine etc. Most of the naturally occurring xanthines possess broad-spectrum of beneficial to human and animal organisms vital functions, and thus constitute very important class of relatively cheap, versatile and sustainable heterocyclic synthons in drug design. The major pharmacological actions of the xanthines are: (i) inhibitory activity against tissue phosphodiesterases (PDEs), (ii) antagonistic properties toward adenosine receptors (A_1 , A_{2A} , A_{2B} and A_3), and (iii) inhibition of the intracellular calcium ions release [1]. In this regard, various synthetic 1,3-dialkylxanthine derivatives are appreciated for their broncho- and vasodilator activity, thereby comprising significant role in treatment of respiratory system (airways) diseases [i.e. chronic obstructive pulmonary disease (COPD) and acute bronchial asthma] as well as cardiovascular dysfunctions (peripheral and cerebral vascular disease, coronary artery disease etc.). Several pharmaceutically relevant compounds with xanthine moiety, including proxiphylline **I**, enprophylline **II**, aminophylline **III**, diprophylline **IV**, xanthinol **V**, bamifylline **VI**, acebrophylline **VII**, doxofylline **VIII**, dasantafile **IX**, furafylline **X**, reproterol **XI**, arofylline **XII** and pentifylline **XIII** have been developed and marketed in the last few decades (Fig. 1). Beside popular broncho- and vasodilators mentioned-above, other small xanthine-like pharmaceutically active molecules with various clinical indications, including pentoxifylline **XIV**, propentofylline **XV**, lisofylline **XVI** and dimenhydrinate **XVII** are sold worldwide with a great financial benefit (Fig. 1).

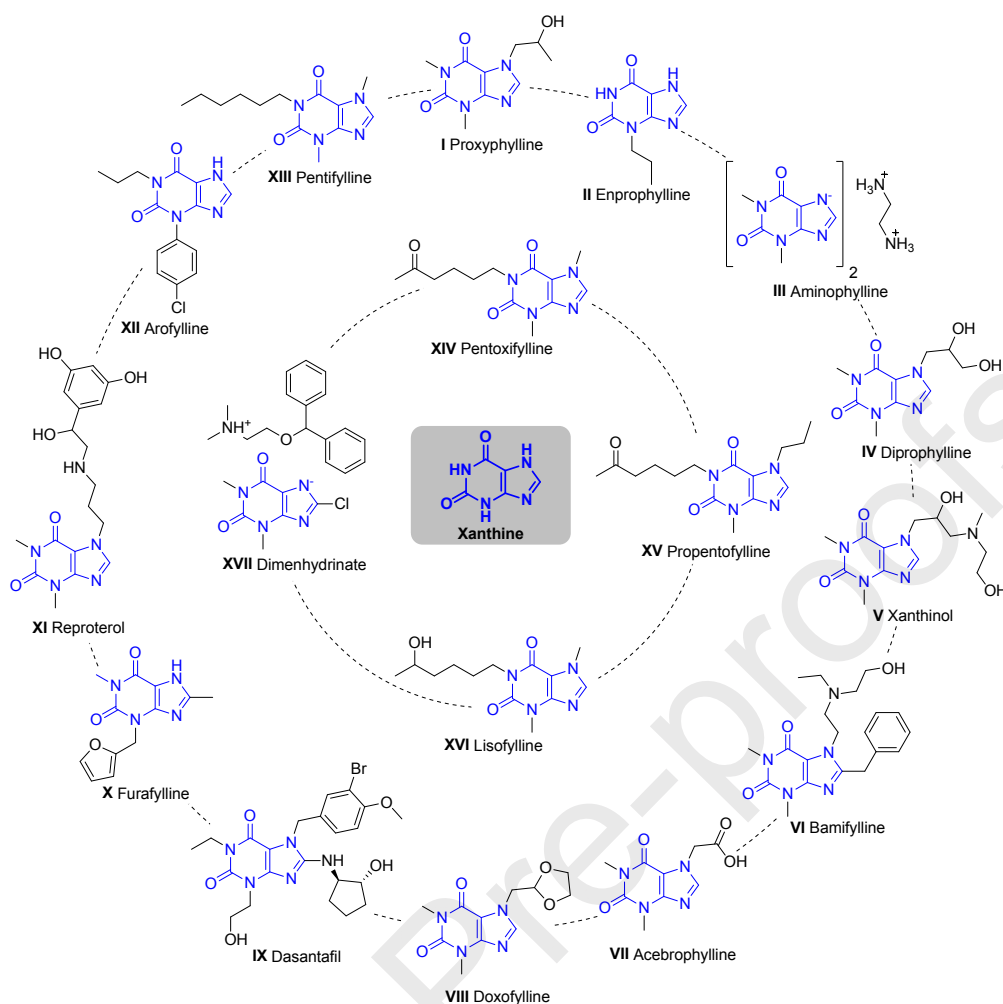


Fig. 1. Examples of the xanthine-based active pharmaceutical ingredients (APIs).

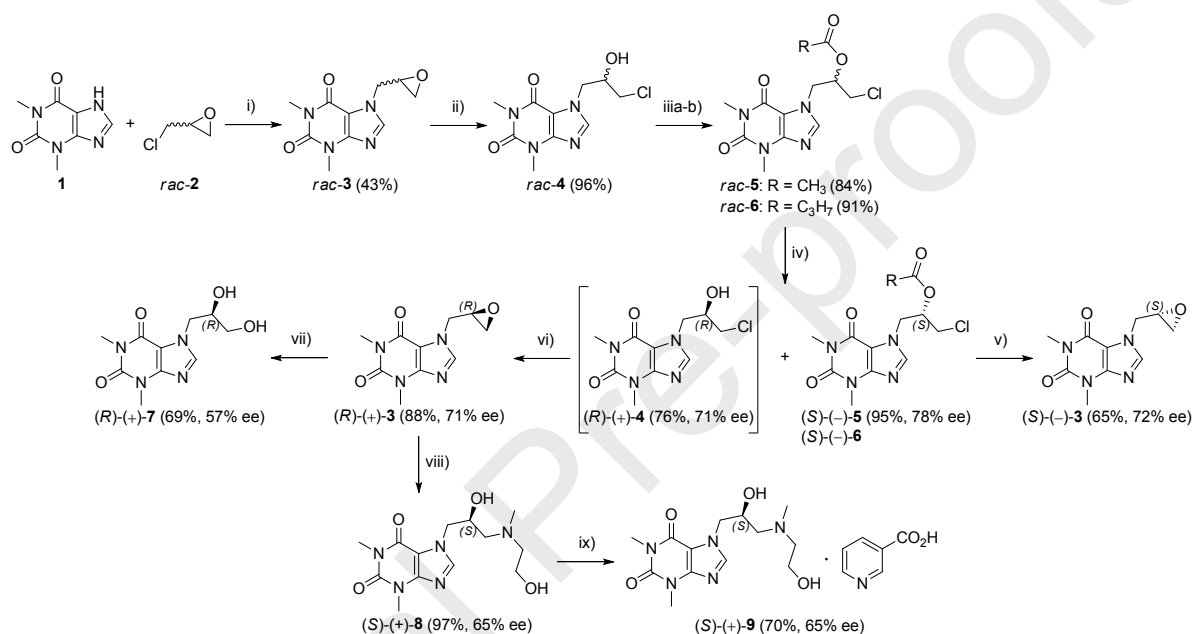
Noteworthy, pharmacologic efficacy and few side effects represented by commercialized APIs depicted in Fig. 1 constitutes a driving force for constant development of novel biologically active compounds with 1,3-dialkylxanthine core structure and relevant medical applications. Obviously, most of these studies focus their efforts toward the synthesis of high affinity and selective A_1 [2–5], A_{2A} [6–10], A_{2B} [11–20] and/or A_3 [21,22] adenosine receptor antagonists as well as selective inhibitors of phosphodiesterase 5 (PDE5) [23]. Although less common, but also highly useful are screening campaigns dedicated to discovery of novel inhibitors of acetylcholinesterase (AChE) [24], monoamine oxidase B (MAO-B) [25,26], and dipeptidyl peptidase 4 (DPP4) [27–29], respectively. In addition, compounds bearing 1,3-dimethylxanthine moiety (subunit) appear to be promising lead structures for the development of anti-HIV [30], anticancer [31], antimicrobial [32,33] and antimycobacterial [34] agents.

Moreover, according to ‘*World Health Statistics 2020*’ WHO report [35], both cardiovascular (CVD) and chronic respiratory diseases (obstructive airways diseases) were responsible for over 21 million deaths worldwide in 2016, and since being leading causes of death in human population next to cancers, they remain one of the greatest public health challenges these days. In order to decrease global cardio/respiratory mortality rate as well as to enhance the patient’s comfort and quality of life, studies on novel therapeutic agents or old drugs with improved pharmacodynamic activities and pharmacokinetic properties tailored to treatment of pulmonary and CV diseases have become an important area in medicinal chemistry.

Taking into account the above-mentioned facts as well as following the line of modern principles concerning restrictions imposed to chiral active pharmaceutical ingredients (APIs) [36,37], here we elaborate on a simple and straightforward preparative chemoenzymatic synthetic route toward enantiomerically enriched broncho/vasodilators, namely diprophylline **IV** and xanthinol nicotinate (nicotinic salt of **V**). To the best of our knowledge until now both these alkylxanthine-related APIs have been synthesized in optically active form only by using classical organic synthetic methods. Unfortunately, previous literature protocols suffers from usage of costly commercial chiral building blocks, such as (*R*)- or (*S*)-3-chloro-1,2-propanediol in the case of enantiomeric diprophylline synthesis [38] or (*S*)-(+)-epichlorohydrin in the case of (*R*)-(-)-xanthinol nicotinate synthesis [39], which may endanger the economic viability of production of these APIs at industrial scale. An optical resolution approach consisting of tedious and low-efficient fractional recrystallization of diastereoisomeric salts formed from racemic xanthinol and (1*S*)-(+)-10-camphorsulfonic acid was also reported [40]. Nevertheless, this methodology except need of performing laborious and time-consuming 5-fold recrystallization of (*R*)-(-)-xanthinol (+)-camphor-10-sulfonate, additionally requires neutralization of acidic moiety coming from resolving agent. The second-mentioned operation is carried out on a column packed with amberlite CG-400 anion exchange resin. Certainly, such a sophisticated removal procedure cause the whole process not amenable to scale-up. Therefore, in continuation to our previous synthetic campaigns devoted to development of chemoenzymatic methods of APIs synthesis [41–43] as well as owing to high enantiomeric resolution efficiency and robustness of lipases in biocatalytic investigations on other pharmaceuticals [44–47] as well as their valuable precursors [48–50], in this paper we expand on novel operationally-simple biotechnological processes of high scientific and industrial importance, which use one common key-intermediate for both of the title products.

2. RESULTS AND DISCUSSION

Herein, we report the results on devising straightforward chemoenzymatic route toward two enantiomeric bronchial vasodilators, namely diprophylline (**7**) and xanthinol nicotinate (**9**), identifying racemic 7-(3-chloro-2-hydroxypropyl)theophylline (*rac-4*) as a valuable precursor for both of them. In this regard, the synthetic pathway of chemoenzymatic asymmetric preparation of non-racemic title APIs consisting of classical enzymatic kinetic resolution (EKR) methodology as a key-step is outlined below (Scheme 1).



Scheme 1. Chemoenzymatic synthesis of enantioenriched diprophylline (**7**) and xanthinol nicotinate (**9**). Reagents and conditions: (i) *rac-2* (6.4 equiv), anh. K_2CO_3 (cat.), DMF, 48 h at 75 °C; (ii) 36% HCl (3 equiv), $CHCl_3$, 1 h at 0–5 °C; (iii-a) Ac_2O (5 equiv), DMAP (0.5 equiv), $CHCl_3$, 1 h at 0–5 °C; (iii-b) butyryl chloride (6.1 equiv), Et_3N (3 equiv), DMAP (0.5 equiv), $CHCl_3$, 24 h at 40 °C; (iv) Novozym 435 (50% w/w), MeOH (10 equiv), CH_3CN , 16 days at 37 °C, 700 rpm; (v) LiOH (2.6 equiv), CH_3CN/H_2O (35:1, v/v), 1.5 h at 0–5 °C, then 24 h at RT; (vi) NaOH (1 equiv), CH_2Cl_2/H_2O (1.6:0.16, v/v), 1 h at 0–5 °C, then 2 h at RT; (vii) 50% H_2SO_4 (pH 1), acetone/ H_2O (7:3, v/v), 2 h at 50–60 °C; (viii) 2-(methylamino)-ethanol (1.2 equiv), 2-PrOH, 1.5 h at reflux; (ix) nicotinic acid (1 equiv), 2-PrOH, 15 min at reflux, 24 h at RT.

2.1. Synthesis of Racemic Substrates.

The required racemic substrates and reference compounds *rac-4–6* for biocatalytic studies were obtained in 2-3-step reaction sequence starting from the corresponding commercially available theophylline (**1**, 1,3-dimethyl-7*H*-purine-2,6-dione) and racemic epichlorohydrin (*rac-2*). In the first step, the synthesis of the racemate *rac-3* was performed by the K_2CO_3 -mediated regioselective ring-opening of *rac-2* with **1** in DMF, which proceeded with moderate 43% yield. The obtained epoxide *rac-3* was subsequently treated with 36% HCl to

afford racemic chlorohydrin *rac-4* in excellent 96% yield. Such an excellent yield was due to facile isolation of the reaction product *rac-4* without necessity of purification step. Noteworthy, although using strong acidic conditions, which may potentially promote formation of undesired regioisomer as a product of oxirane-ring opening of *rac-3* at the sterically more hindered electrophilic carbon atom [51], the reaction carried out in an ice-cold CHCl_3 solution led exclusively to alcoholic product *rac-4* possessing secondary hydroxyl group according to NMR indications. Next, the respective racemic acetate *rac-5* and butyrate *rac-6* have been obtained through a simple DMAP-catalyzed esterification procedure. However, treatment of *rac-4* with 1.2 equiv of acetic anhydride or butyric chloride in the presence of 1.3 equiv of triethylamine (Et_3N) and catalytic amount of 4-dimethylaminopyridine (DMAP) in CH_2Cl_2 failed as the substrate conversions were very low. Therefore, to increase the reaction rate of the ester formation the conditions were slightly modified in terms of the solvent (an improvement of substrate's solubility was observed using CHCl_3) and the molar excess of acylating reagents used in respect to *rac-4*. When 5-fold molar excesses of Ac_2O relative to the substrate was employed the DMAP-catalyzed acetylation of *rac-4* proceeded smoothly even without using additional amount of Et_3N as a base, and the desired product *rac-5* was prepared in very good 85% yield after only 1 h of stirring the reaction at 0–5 °C. Unexpectedly, under optimized reaction conditions the reactivity of *rac-4* toward butyryl chloride was still significantly limited, and to obtain *rac-6* with acceptable yield the reaction time was elongated up to 24 h and the temperature was increased from 5 to 40 °C searching for improving the reactivity. Hopefully, the performed adjustments resulted in the formation of butyrate *rac-6* in excellent 91% yield.

2.2. Lipase-Catalyzed KR of Racemic Substrates.

The next step was to develop synthesis of optically active valid intermediates for the titled APIs. High catalytic activity and stereoselectivity of lipases in the classical kinetic resolution (KR) of secondary alcohols [52–56] as well as our successfully developed biocatalytic method toward efficient synthesis of proxyphylline (**I**) enantiomers reported previously [42], prompted us to undertake two independent strategies for the preparation of enantioenriched chlorohydrin **4**: (i) the lipase-catalyzed enantioselective transesterification of *rac-4* with vinyl esters as the acyl group donor reagents; and (ii) the lipase-catalyzed hydrolytic resolution of the corresponding esters *rac-5* and *rac-6*. In this regard a considerable number of commercially available lipase preparations manufactured from different microorganisms (see

Supporting Information) were tested in both synthetic modes, but none of them was able to efficiently catalyze the desired reactions. Since traces of product were detected after one day of conducting KR with lipase type B from *Candida antarctica* immobilized on acrylic resin (CAL-B, Novozym 435), and because it was previously proved by us that CAL-B is particularly efficient on xanthine-based substrates, we further concentrated our efforts on optimization of the CAL-B-catalyzed processes. Unfortunately, no significant activity was observed when using other commercial CAL-B preparations occurring both in native (Lipozyme CALB L) and immobilized form (Chirazyme L-2, C-2, Lipozyme 435, CAL-B-Immobead 150). This might be due to very limited solubility of xanthine derivatives in standard organic solvents that are biocompatible with enzymes and conventionally used in the lipase-catalyzed reactions. When facing such limitations, it must be taken into account that even negligible differences in lipases' form among one particular type, deriving i.e. from method of immobilization and/or the type of enzymes carriers, can affect not only physical, chemical and mechanical properties of such preparations, but also may significantly influence their catalytic behaviour. Moreover, after detailed evaluation of solubility of racemic substrates *rac-4*, *rac-5*, and *rac-6* [see Supporting Information (Table S5)] in various organic media, we realized that manipulations with those compounds in EKR manner would constitute a significant drawback for reactions' outcome in terms of the rate and stereoselectivity. As a matter of fact, our concerns about difficult biotransformations of the xanthine derivatives were substantiated very soon.

2.2.1. Lipase-Catalyzed KR of *rac-4* Using Enantioselective Transesterification.

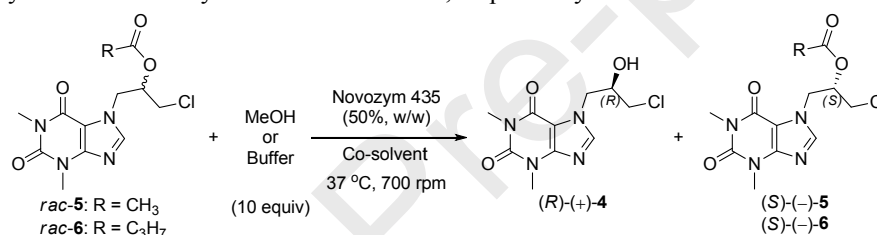
At first, we have attempted analytical scale (Novozym 435)-catalyzed transesterification experiments by screening enol esters (vinyl acetate and vinyl butanoate) as acyl group donors and several organic solvents as reaction medium, including polar one (1,4-dioxane, CH₃CN, acetone, THF) and relatively semi-polar (CH₂Cl₂, CHCl₃), within which *rac-4* formed homogenous solution. It is worth mentioning that working with vinyl esters has the great advantage of avoiding major two problems regarding: (i) necessity of reaction work-up as well as reversibility of esterification processes [as the generated by-product (vinyl alcohol) spontaneously tautomerizes *in situ* to a stable carbonyl compound (acetaldehyde), which is unable to attend in backward reaction (hydrolysis of ester)]. Unfortunately, it turned out that the examined EKRs failed when using enzymatic systems composed of single-solvent reaction media, resulting in the comparatively low conversions after 7 days. This is in

contradiction to our previous results on the kinetic resolution of racemic proxyphylline (**I**) [42], which were feasible to perform with at least moderate enantioselectivities in the case of both solvents listed-above (CHCl_3 or CH_3CN). The rest of the organic solvents commonly used in lipase-catalyzed reactions (i.e. TBME, DIPE, toluene, *tert*-amyl alcohol etc.) also failed due to mass transfer limitations typical for biphasic systems, which additionally impaired the diffusion of the substrate molecules *rac*-**4** to reach the enzyme active site. Moreover, this phenomena shows how minor differences in the structure of racemic substrates can determine the activity and selectivity of lipase catalysts. At first glance, *rac*-**4** and proxyphylline (**I**) appears to be very similar in terms of the chemical structure, however, the preliminary set of experiments revealed that additional chlorine atom positioned at terminal methylene group in aliphatic side-chain of the substrate *rac*-**4** can drastically quell catalytic potency of the studied lipases. Interestingly, in successive runs (not shown herein), we have observed some rate improvement upon using two-component reaction media. In this regard, when resolving enantiomers of *rac*-**4** with vinyl esters under kinetically-controlled conditions mediated by Novozym 435 suspended in a mixture of $\text{CH}_3\text{CN}/\text{CHCl}_3$ (5:1, v/v) slightly improved reactivity and selectivity toward the formation of the (*R*)-esters were attained (up to $E=9$, 39% conv.). All analytical-scale enzymatic reactions were performed with 3 equiv of vinyl esters as the acyl-transfer-reagents at 37 °C for at least 7 days. In the case of vinyl acetate, (Novozym 435)-catalyzed enantioselective transesterification of *rac*-**4** yielded ester (*R*)-(+)-**5** in 71% ee and unreacted (*S*)-**4** recovered with 45% ee. In turn, while using vinyl butanoate the desired EKR products were obtained with considerably lower enantiomeric purities as the formed optically active butanoate (*R*)-(+)-**6** was isolated with 34% ee and the remaining (*S*)-(–)-**4** in 22% ee. Furthermore, it has to be pointed out that in order to establish optical purity of butanoate (*R*)-(+)-**6** this compound had to be hydrolyzed using 20-fold molar excess of NaOH dissolved in MeOH, as the HPLC baseline resolution for the racemic analytical standard of this compound *rac*-**6** could not be afforded with the available chiral columns and elution conditions. The another drawback of the reaction with vinyl butanoate was the problem with estimation of conversion rate owing to thermal decomposition of (*R*)-(+)-**6** during gas chromatography. However, the conversions of lipase-mediated enantioselective *O*-acylation of *rac*-**4** after 7 days were only 39% and the values of *E*-factor (2–9) were too low for achieving a high enantiomeric excesses of the resolution products, thus further investigations with vinyl esters were abandoned as being non-preparative from the synthetic point-of-view.

2.2.2. Enantioselective Lipase-Catalyzed KR of *rac-5* and *rac-6* – Hydrolysis vs Alcoholysis.

Since we were interested in development of selective transformations, and because of the known higher reactivity and selectivity of lipases in enzyme-mediated hydrolysis of esters, therefore it was worthwhile to investigate also hydrolysis of the respective esters. Toward this goal, we explored the EKR of both racemic esters *rac-5* and *rac-6* under various hydrolytic conditions. In this context, several pivotal reaction's parameters were thus varied, such as: (i) time of the process, the type of (ii) racemic substrate (acetate *rac-5* vs butanoate *rac-6*), and (iii) acyl group acceptor (water vs various aliphatic alcohols), as well as (iv) type and concentration of aqueous buffer, and (v) the addition of organic co-solvent. The most representative experimental details of this optimization are collected in Table 1.

Table 1. Examination of the analytical-scale (Novozym 435)-catalyzed KR conditions for the enantioselective hydrolysis and methanolysis of *rac-5* and *rac-6*, respectively.



Entry	Compound	Nucleophile	Co-solvent	<i>t</i> [d]	Conv. ^a [%]	ee _s ^b [%]	ee _p ^b [%]	<i>E</i> ^c
1	<i>rac-5</i>	1 M THB ^d	CHCl ₃	1	0	N.D. ^e	N.D. ^e	N.D. ^e
2		0.1 M THB ^f	CHCl ₃	1	0	N.D. ^e	N.D. ^e	N.D. ^e
3		0.1 M THB ^f	Dioxane	7	0	N.D. ^e	N.D. ^e	N.D. ^e
4		0.1 M PPB ^g	Dioxane	7	14	1	6	1
5		MeOH ^h	Dioxane	4	26	27	77	10
6		MeOH ^h	CH ₃ CN	4	50	65	64	9
7		MeOH ^h	CH ₃ CN	7	49	64	67	10
8	<i>rac-6</i>	1 M THB ⁱ	CHCl ₃	1	0	N.D. ^e	N.D. ^e	N.D. ^e
9		0.1 M THB ^j	CHCl ₃	1	0	N.D. ^e	N.D. ^e	N.D. ^e
10		0.1 M THB ^j	Dioxane	7	0	N.D. ^e	N.D. ^e	N.D. ^e
11		0.1 M PPB ^k	Dioxane	7	22	2 ^l	7	1
12		MeOH ^m	Dioxane	4	25	4 ^l	12	1
13		MeOH ^m	CH ₃ CN	4	33	16 ^l	33	2

^a Calculated from the enantiomeric excess of the unreacted acetate (ee_s) and the product (ee_p) according to the formula $\text{conv.} = \text{ee}_s / (\text{ee}_s + \text{ee}_p)$.

^b Determined by chiral HPLC analysis by using a Chiralcel OD-H column.

^c Calculated according to Chen et al. [57], using the equation: $E = \{ \ln[(1 - \text{conv.})(1 - \text{ee}_s)] / \ln[(1 - \text{conv.})(1 + \text{ee}_s)] \}$.

^d Conditions: *rac-5* 50 mg, lipase 10 mg, solvent 1.0 mL, 1 M Tris-HCl Buffer (pH 8.2) 0.5 mL, 37 °C, 700 rpm (magnetic stirrer).

^e Not determined due to low reaction rate.

^f Conditions: *rac-5* 50 mg, lipase 25 mg, solvent 0.9 mL, 0.1 M Tris-HCl Buffer (pH 7.5) 1.0 mL, 37 °C, 700 rpm (magnetic stirrer).

^g Conditions: *rac-5* 50 mg, lipase 25 mg, solvent 0.9 mL, 0.1 M (KH₂PO₄/K₂HPO₄) Potassium Phosphate Buffer (pH 7.5) 1.0 mL, 37 °C, 700 rpm (magnetic stirrer).

^h Conditions: *rac-5* 50 mg, lipase 25 mg, solvent 1.0 mL, MeOH 51 mg, 64 μL (10 equiv), 37 °C, 700 rpm (magnetic stirrer).

ⁱ Conditions: *rac-6* 50 mg, lipase 10 mg, solvent 1.0 mL, 1 M Tris-HCl Buffer (pH 8.2) 0.5 mL, 37 °C, 700 rpm (magnetic stirrer).

^j Conditions: *rac-6* 50 mg, lipase 25 mg, solvent 0.9 mL, 0.1 M Tris-HCl Buffer (pH 7.5) 1.0 mL, 37 °C, 700 rpm (magnetic stirrer).

^k Conditions: *rac-6* 50 mg, lipase 25 mg, solvent 0.9 mL, 0.1 M (KH₂PO₄/K₂HPO₄) Potassium Phosphate Buffer (pH 7.5) 1.0 mL, 37 °C, 700 rpm (magnetic stirrer).

^l Determined by HPLC after chemical methanolysis of butanoate (*S*)-(-)-6 into (*S*)-(-)-4.

^m Conditions: *rac-6* 50 mg, lipase 25 mg, solvent 1.0 mL, MeOH 47 mg, 59 μL (10 equiv), 37 °C, 700 rpm (magnetic stirrer).

Again, encouraged by our positive experiences with synthesis of enantiomeric proxyphylline (**I**) [42], at first we tried to apply very similar conditions toward racemates *rac-5* and *rac-6* used in this project. Unfortunately, it turned out that the adopted strategy failed because of the limited solubility of both the employed substrates *rac-5* and *rac-6* in the model homogeneous reaction medium composed of 1 M Tris-HCl Buffer (pH 7.5)/CH₃CN mixture. To enhance solubility of the racemic esters, we decided to change the co-solvent from CH₃CN to CHCl₃. To our disappointment, first attempted reactions (Table 1, entry 1 and 8) showed no detectable conversions. As we presumed that it might be due to a high-molarity of Tris buffer, we decided to decrease its concentration from 1 M to 0.1 M, and repeated the reaction in CHCl₃. Also this time no progress of the reaction was observed (Table 1, entry 2 and 9), and we came to the conclusion that the reason might be two-fold: on the one hand the halogenated solvents mostly decrease the enzymes' activity, and on the other hand, the external mass transfer and diffusion of the substrate *rac-4* molecules into the lipase active-site can be deteriorated by immiscibility of both the employed aqueous and organic phases, and thus taken together limit the overall reaction rate. Failures at this stage forced us to turn our attention toward homogeneous reaction medium instead of biphasic hydrolytic conditions. In this regard, a mixture of miscible co-solvents, 1,4-dioxane and 0.1 M Tris-HCl Buffer (pH 7.5), was examined. Unfortunately, the desired reaction product was not detected even after significant prolongation of the reaction time up to 7 days (Table 1, entry 3 and 10). Then, we changed the type of an aqueous buffer solution from Tris-HCl to 0.1 M KH₂PO₄/K₂HPO₄ buffer (pH 7.5), and repeated the enzymatic reaction in 1,4-dioxane. This time, the reactions hopefully proceeded, however, very poor conversions (14–22%) and enantioselectivities (up to *E*=1) were observed for both the resolved substrates (Table 1, entry 4 and 11). The (Novozyme 435)-mediated hydrolytic EKR of *rac-5* in solution of potassium phosphate buffer/1,4-dioxane could barely reach 14% conv. after 7 days, thus furnishing the products (*R*)-(+)-**4** and (*S*)-(–)-**5** in almost racemic form (<6% ee). Very similar results in terms of stereochemical outcome were obtained by EKR of *rac-6*, which yielded (*R*)-(+)-**4** with extremely low 2% ee and (*S*)-(–)-**6** in 7% ee with 22% conv. We found those derivatives much more challenging as a substrates for biocatalysis than proxyphylline, and thus needed further advanced investigations.

In the next step, we changed the synthetic strategy into lipase-catalyzed enantioselective alcoholysis. Working in such mode, without presence of water, is generally more beneficial than classical aqueous buffer-promoted hydrolysis as after completion of the reaction the enzyme can be removed by simple filtration and the filtrate progressed directly to

chromatographic separation without an intermediate extraction step. Initially, we have examined (Novozym 435)-catalyzed EKR of both racemic esters *rac-5* and *rac-6* under influence of 10-fold molar excess of MeOH as the nucleophile in 1,4-dioxane at 37 °C. When terminating the reactions after 4 days we could finally noticed an improvement of the rates, however, still the conversions were very low in the range of 25–26% (Table 1, entry 5 and 12). When comparing both attempts, it was obvious that significantly more efficient in terms of enantioselectivity was EKR of *rac-5* ($E=10$) than *rac-6* ($E=1$). An enantioselective methanolytic kinetic resolution mediated by Novozym 435 resulted in the formation of optically active chlorohydrin (*R*)-(+)-**4** with acceptable 77% ee and unreacted acetate (*S*)-(–)-**5** in 27% ee. Unexpectedly, a simultaneously performed studies on slightly different catalytic system composed of Novozym 435 suspended in a mixture of MeOH (10 equiv)/CH₃CN resulted in the formation of (*R*)-(+)-**4** with 50% conv. for resolution of *rac-5* and 33% conv. for *rac-6* after 4 days (Table 1, entry 6 and 13). Gratifyingly, the most promising enzymatic methanolysis results concerning chirality inducement were obtained with *rac-5* as the substrate, thus affording enantiomerically enriched product (*R*)-(+)-**4** with 64% ee, and the remaining acetate (*S*)-(–)-**5** with 65% ee (Table 1, entry 6). As it is well-known that exceeding EKR conversion above 50% enhance the optical purity of the slower reacting enantiomer, we decided to evaluate how elongation of the reaction time would influence the resolution outcome in favor of (*S*)-(–)-**5**. To our disappointment, when the EKR of *rac-5* was stopped after as long as 7 days we found that the recovered (*S*)-(–)-**5** was provided with slightly deteriorated enantiomeric excess (64% ee), and its deacetylated counterpart (*R*)-(+)-**4** in enantioenriched form characterised by 67% ee (Table 1, entry 7). Notably, it became obvious that elongation of the EKR process was detrimental as the transformations went to completion after 4 days. The other serious drawback of using methanol in lipase-catalyzed alcoholysis of esters is inactivation of the enzyme due to stripping of the water molecules from the protein surface. In an aim to investigate the enzymatic alcoholysis more deeply and counteract negative influence of methanol, in a consecutive step we employed different aliphatic alcohols as acyl-group-acceptors, that were as follows: 1-propanol, 1-butanol, 1-pentanol, and 1-heptanol (all of them used with 10 equiv). Nevertheless, neither of them gave satisfactory results concerning the rate acceleration and the conversion. Interestingly, again when performing EKR of *rac-5* under the optimized operational conditions with other CAL-B preparations, it turned out that the kinetic resolutions were catalyzed only by Novozym 435, and the other tested enzymes were inactive toward *rac-5* or the conversion rates were negligible. After the described analytical-scale experiments it may be noted, that among

various reaction parameters, especially enzyme source, form of the enzyme preparation as well as an organic co-solvent addition and type of acyl-group acceptor can have a significant impact on the biocatalytic effectiveness of EKR of xanthine-like derivatives.

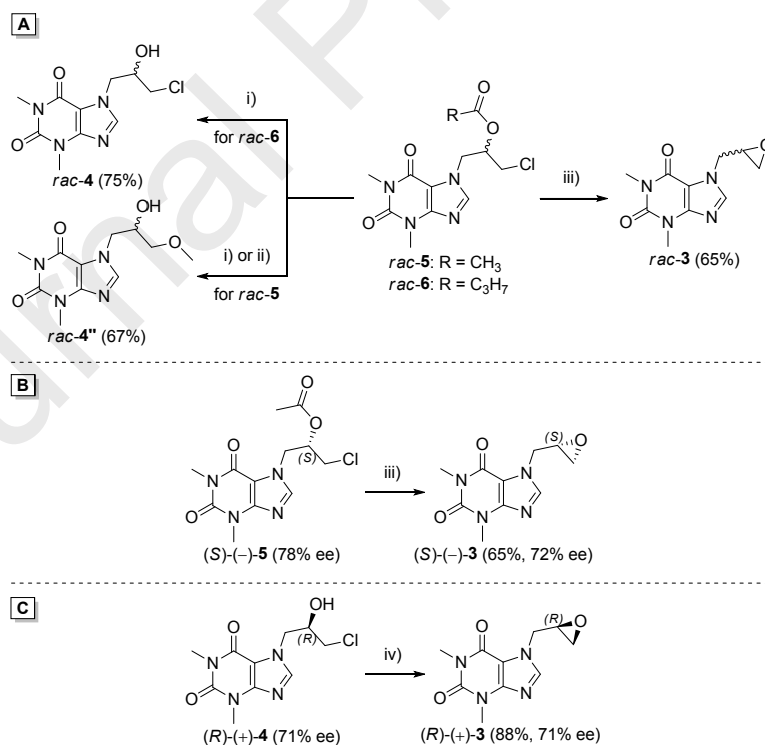
Although the enzymatic reactions were sluggish and determined with moderate resolution efficiency, our next step was capitalization on the scalability and robustness of this method in a half gram-scale reactions. Upon subsequent scale-up, pleasantly, the EKR process took place with increased enantioselectivity ($E=14$), 52% conv. and enantiomeric enrichment of both resolution products, reaching accordingly 71% ee for optically active chlorohydrin (*R*)-(+)-**4**, and 78% ee for the residual acetate (*S*)-(–)-**5**. The separation of the resolution products on a silica gel column revealed that the formed alcohol (*S*)-(–)-**4** could be isolated in high 76% yield, and the unreacted acetate (*S*)-(–)-**5** in excellent 95% yield, corresponding closely to the theoretical 52% proportions of the enantiomers in the racemate. However, one must be pointed out herein, the resolutions on a bigger scale lasted as long as for 16 days even using Novozym 435 with 50% w/w in ratio to substrate *rac*-**5**. In the light of this finding, it became clear that this process proved to be moderately flexible for being up-scaled in a straightforward manner, and definitely needed some additional modifications. With the hope of shortening the time of the product formation, we thereby performed the reactions under microwave irradiation conditions. These experiments have shown that lipase-catalyzed KR proceeded unsuccessfully, and since applying microwave radiation for a couple of hours resulted only in the recovery of unreacted *rac*-**5** this protocol was no further studied.

2.3. Approaches to the Preparation of Enantiomeric APIs – 7, 8, and 9.

In the project continuation we searched for the optimal reaction conditions for base-mediated ring-closure reaction of the halohydrin moiety present in the enzymatically resolved products, that are: (*R*)-(+)-**4** (71% ee) and (*S*)-(–)-**5** (78% ee). At first, to obtain both enantiomers of non-racemic chlorohydrin **3**, we focused our efforts on deprotection procedure of the acetate group installed in (*S*)-(–)-**5** (Scheme 2B). Initial experiments were performed with racemic acetate *rac*-**5** by using the same reaction conditions as NaOH-mediated methanolysis of butanoate (*R*)-**6** (see section 2.2.1.). Unexpectedly, the removal of an acetate moiety resulted in the formation of undesired ethereal product *rac*-**4**” isolated in 67% yield and fully characterized by spectroscopic analyses (Scheme 2A, see also Supporting Information). Apparently, this was the consequence of employing a huge excess of NaOH (20 equiv) in MeOH, which in this case promoted a sequence of the following transformations: (i)

hydrolysis of an ester *rac-5* to yield *rac-4*, (ii) the epoxide-ring forming intramolecular nucleophilic substitution of the chlorine atom with hydroxyl group in *rac-4* to yield *rac-3*, and subsequent (iii) nucleophilic oxirane-ring opening in *rac-3* with sodium methoxide/methanol to yield *rac-4''*. What is even more compelling, when decreasing amount of the NaOH to 3 equiv and temperature from 37 °C to 0–5 °C, the reaction failed as well, resulting in isolation of undesired by-product. This forced us to exclude MeOH as nucleophile and employ weaker base than NaOH. Finally, when the reaction of (*S*)-(–)-**5** was carried out with 2.6 equiv of LiOH in a mixture of CH₃CN/H₂O for 24 h at room temperature, the sequential cleavage of the acetyl group and ring closure were afforded in one-pot strategy to obtain (*S*)-(–)-**3** in 65% yield (Scheme 2B). The developed procedure was simple and rather efficient, however, partial racemisation of optically active epoxide (*S*)-(–)-**3** occurred as it was isolated with 72% ee.

In turn, enantiomeric chlorohydrin (*R*)-(+)-**4** obtained *via* lipase-catalyzed EKR was transformed directly into the corresponding epoxide (*R*)-(+)-**3** using an equimolar amounts of NaOH in the appropriate CH₂Cl₂/H₂O mixture for overall 3 h of stirring the reaction mixture at cool to ambient temperature. This attempt resulted in the formation of (*R*)-(+)-**3** in very high 88% yield and without loss of the optical purity (71% ee) (Scheme 2C).



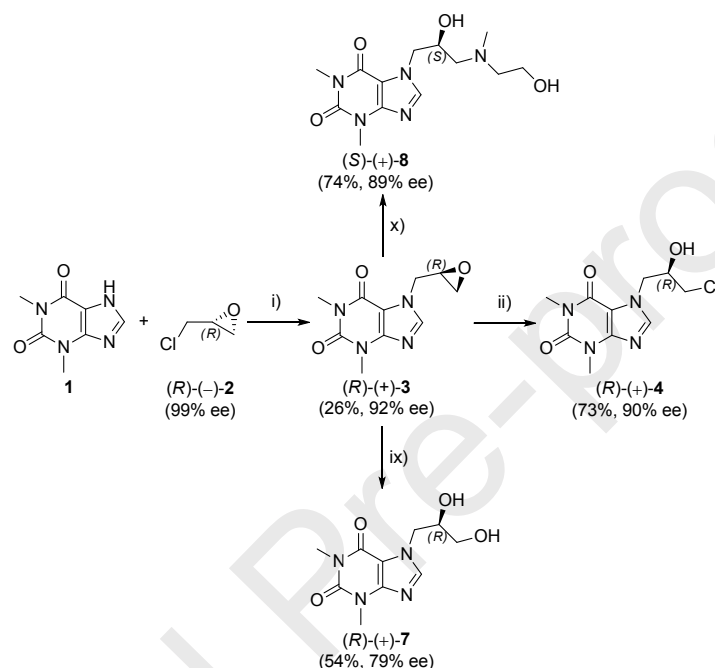
Scheme 2. Attempts at base-catalyzed hydrolysis of esters *rac-5*, *rac-6*, (*S*)-(–)-**5** and ring-closure in (*R*)-(+)-**4**. Reagents and conditions: (i) NaOH (20 equiv), MeOH, 2 h at 37 °C; (ii) NaOH (3 equiv), MeOH, 24 h at 0–5 °C; (iii) LiOH (2.6 equiv), CH₃CN/H₂O (35:1, v/v), 1.5 h at 0–5 °C, then 24 h at RT; (iv) NaOH (1 equiv), CH₂Cl₂/H₂O (1.6:0.16, v/v), 1 h at 0–5 °C, then 2 h at RT.

As both the antipodes of intermediate chiral epoxide **3** were obtained with a similar enantioenrichment (ca. 72% ee), the rest of the planned synthetic pathway was realized starting with only one of them. In this regard, independent experiments conducted with (*R*)-(+)-**3** were performed to afford both non-racemic title APIs – diprophylline (**7**) and xanthinol nicotinate (**9**). At first, we decided to synthesize enantiomeric diprophylline (**7**) by utilizing an aqueous base solutions. Unfortunately, neither NaOH nor K₂CO₃ dissolved in H₂O were efficient in this approach. Next, acid-mediated ring opening reaction toward (*R*)-(+)-**3** was applied. Upon heating of (*R*)-(+)-**3** in a mixture of 50% H₂SO₄ and acetone/H₂O at 50–60 °C for 2 h, it underwent hydrolysis of its oxirane-ring with partial loss of optical purity ($\Delta\%$ ee = 14), thus affording (*R*)-(+)-**7** in 69% isolated yield and with moderate 57% ee. The synthesis of second API molecule was slightly more efficient as the reaction of (*R*)-(+)-**3** with 1.2-fold molar excess of 2-(methylamino)-ethanol carried out in boiling 2-PrOH for 1.5 h furnished enantiomerically enriched xanthinol [(*S*)-(+)-**8**] in an excellent (almost quantitative) 97% isolated yield and with 65% ee according to chiral HPLC. In view of this findings, it was clear that during epoxide-ring opening reactions the basic conditions promote racemisation with lower degree as the drop in enantiomeric excess was less detrimental for optical purity of (*S*)-(+)-**8** ($\Delta\%$ ee = 6). The final synthetic step of the preparation of enantiomerically enriched xanthinol nicotinate [(*S*)-(+)-**9**] was accomplished by stirring an equimolar mixture of (*S*)-(+)-**8** and nicotinic acid in boiling 2-PrOH for 15 min, after which the agitation was continued for 24 h at room temperature. In this manner, and after subsequent simple work-up the nicotinic salt of title API (*S*)-(+)-**9** was afforded in 70% yield and 65% ee.

2.4. Determination of Reactions' Stereochemistry.

In order to verify the stereochemistry of the performed enzymatic reactions as well as other chemical transformations performed in these studies, the assignment of absolute configuration of the respective products is pivotal. Of course, in some extent this task has been simplified since the absolute configuration of optically active xanthinol (**8**) and xanthinol nicotinate (**9**) have already been determined by Grace and co-workers [40]. In turn, both enantiomers of diprophylline (**7**) were synthesized from readily available commercial chiral building block of a defined stereochemistry by Brandel et al. [38], however with great harm to scientific data authors of this publication did not linked the absolute configurations of enantiomeric API **7** with specific rotation signs of its enantiomers. Moreover, for unknown reasons the optical rotation values themselves for nonracemic diprophylline (**7**) have not been reported

previously. Therefore, it was reasonable to fill all those substantial knowledge gaps and follow the tactics concerning correlation by asymmetric synthesis. In this purpose, we have used commercially available enantiomerically pure (*R*)-configured epichlorohydrin [(*R*)-(-)-**2**] to obtain analytical standards for the comparison of the specific rotation signs as well as peaks' elution order of chiral high-performance liquid chromatography (*C*-HPLC) analyses. The respective chemical synthesis route is presented in Scheme 3.



Scheme 3. Synthesis of enantiomerically enriched diprophylline [(*R*)-(+)-**7**] and xanthinol [(*S*)-(+)-**8**]. Reagents and conditions: (i) (*R*)-(-)-**2** (3 equiv), anh. K_2CO_3 (cat.), DMF, 48 h at 75 °C; (ii) 36% HCl (3 equiv), $CHCl_3$, 1 h at 0–5 °C; (ix) 50% H_2SO_4 (pH 1), acetone/ H_2O (7:3, v/v), 2 h at 50–60 °C; (x) 2-(methylamino)-ethanol (1.2 equiv), 2-PrOH, 1.5 h at reflux.

Most of the reaction conditions were almost the same as in **2.1** (see Scheme 1) except for the first step of the repeated synthesis, during which reduced by-half amount of costly non-racemic chlorohydrin (*R*)-(-)-**2** (3 equiv) was applied. Accordingly, the yield of the synthesized epoxide (*R*)-(+)-**3** reached only 26% what constituted almost two-fold worst result when compared to previously performed reaction with *rac*-**2**. Furthermore, in accordance to indications of HPLC equipped with chiral column the enantiomeric purity of (*R*)-(+)-**3** was acquired with very good 92% ee. However, this attempt revealed that basic conditions are unfavorable for stereochemical transformation of **1** into (*R*)-(+)-**3**, thus indicating that competitive S_N2 nucleophilic substitution at C-atom directly bonded to the chloride leaving group in epichlorohydrin [(*R*)-(-)-**2**] occurs as well (the product was formed by direct displacement of the chloride ion). Nevertheless, a competition between substitution

at C-1 and ring-opening at C-3 during the nucleophilic attack performed by the theophylline (**1**) was not a major problem for us, and even provided helpful hint during peaks identification in the HPLC chromatograms. Besides lack of datasets concerning established stereochemistry of non-racemic epoxide **3**, literature suffers from analytical characteristics of optically active 7-(3-chloro-2-hydroxypropyl)theophylline (**4**). To address this issue, we have subjected (*R*)-(+)-**3** into reaction of regioselective epoxide-ring opening with concentrated HCl in ice-cold CHCl₃ to afford (*R*)-(+)-**4** in 73% yield and 90% ee. To our surprise, under the applied reaction conditions deterioration of an optical purity was negligible in this case, reaching only 2%-points loss in the enantiomeric excess values.

Next, under previously established reaction conditions we treated key epoxide intermediate (*R*)-(+)-**3** respectively with H₂SO₄ in aqueous-acetone solution to afford (*R*)-(+)-**7** in 54% yield, and with 2-(methylamino)-ethanol in 2-PrOH to furnish (*S*)-(+)-**8** in 74% yield. Consequently, application of strong acidic conditions gave almost the same significant loss of enantiomeric purity ($\Delta\% ee = 13$) as described before since the synthesis of optically active diprophylline [(*R*)-(+)-**7**] has been accomplished with 79% ee. In turn, drop of the enantiomeric excess during functionalization of (*R*)-(+)-**3** toward optically active xanthinol [(*S*)-(+)-**8**] was less detrimental for stereochemical outcome of this reaction ($\Delta\% ee = 2$), and thus desired API molecule was attained with 89% ee.

In addition, the validity of the correlative approach toward the absolute configuration assignment of chiral compounds was undeniably established by solving X-ray crystal structures for the respective APIs' single crystals. At first, from the anomalous dispersion effect analysis based on the X-ray diffraction experiment, we confirmed that non-racemic diprophylline [(+)-**7**] molecule is actually the (*R*)-(+)-**7** (Fig. 2).

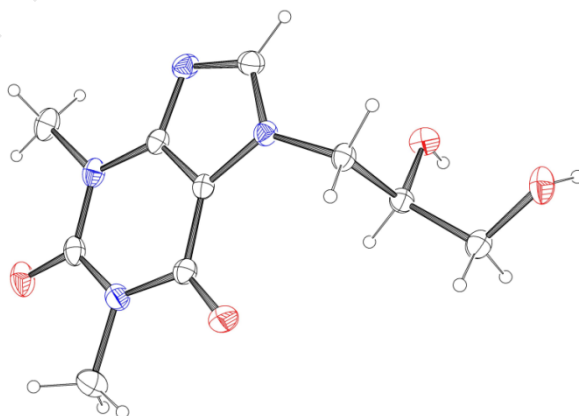


Fig. 2. An ORTEP plot of optically active (*R*)-(+)-**7**. Thermal ellipsoids were drawn at 50% probability (C black, H gray, N blue, O red). The following crystal structure has been deposited at the Cambridge Crystallographic Data Centre and allocated the deposition number CCDC-1815550.

It is somehow interesting that although xanthinol (**8**) has been widely used in clinical practice for over few decades mainly in the form of its' nicotinic acid salt **9** marketed as a racemic solid under various brand names (Complamina[®], Sadamin[®], Nicoplamin[®] etc.), the crystal structures obtained from single-crystal X-ray experiments have not been reported until now. Therefore, to fill this gap trials to grow single crystals of the synthesized optically active xanthinol nicotinate [(+)-**9**] were carried out. After several attempts, crystals with sufficient quality for single-crystal X-ray diffraction analysis were obtained using conventional vapor diffusion crystallization technique (VDCT) employing *n*-hexane as the precipitant. Thus, we could finally indisputably determine the crystal structure of (+)-**9** to be (*S*)-(+)-**9** (Fig. 3).

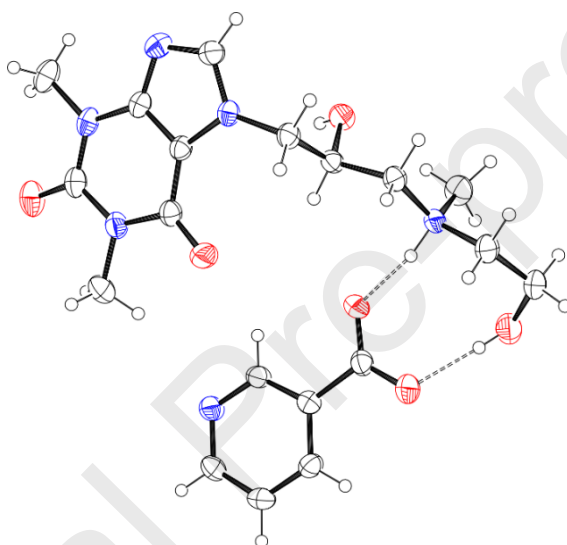


Fig. 3. The asymmetric unit of optically active (*S*)-(+)-**9** showing the formation of the ionic pair. Thermal ellipsoids were drawn at 50% probability (C black, H gray, N blue, O red). The following crystal structure has been deposited at the Cambridge Crystallographic Data Centre and allocated the deposition number CCDC-2016376.

What is important, crystal structure analysis of (*S*)-(+)-**9** reveals that hydrogen atom is exchanged between the nicotinic acid and the xanthinol molecule. Thus, the asymmetric unit is composed of nicotinate anion and xanthinol cation forming an acid···aminoalcohol heterosynthon $R_2^2(9)$ ring via two synergistic N-H···O and O-H···O hydrogen bonds. Observed hydrogen bonds belong to the separate class of doubly ionic H-bond occurring between cations and anions. The ionic charge significantly enhances “charge-assisted” hydrogen bond strength which could be approximate to 5–35 kcal/mol, even up to a third of the strength of covalent bonds. This should be important in bioenergetics including protein folding, enzyme active centers modeling, and biomolecular recognition [58]. Despite most of the additional binding energies compared with general hydrogen bonds come from the electrostatic attraction, an extra contribution could be assigned to the assistance of resonance.

It has already been reported by Beck et al. [59] that very strong hydrogen bonds mostly originate from the classical dipole-dipole attraction as the resonance redistributes the electron density and increases the dipole moments in particular monomers, and are indeed predominantly covalent rather than electrostatic. This covalent character of resonance-assisted hydrogen bonds observed in a charged structure of (+)-**9** has also been proven by Fourier transform mass spectrometry (FTMS). In this case, electronegative FTMS spectrum revealed that for the sample of (+)-**9** the only mass that was found ($[M-H]^-$ 433.1840) corresponded to the total mass of both bounded together components of the API molecule ($C_{19}H_{25}N_6O_6^-$), that is xanthinol and nicotinate ions, whereas the FTMS peaks with a mass referring to individual/separate ionic counterparts have not been detected. It is worth notice, that formation of persistent ion pairs stabilizes the formation of the second pseudo-asymmetric stereogenic center at the nitrogen atom of 2-(methylamino)-ethanol substituent caused by inhibition of the effect of the so-called 'umbrella inversion' of the amine functionality owing to the very strong interaction that occurred between quaternary N-atom and nicotinate counter ion in the formed ion pair present in (+)-**9**.

In the crystal of (*S*)-(+)-**9**, adjacent electroneutral units tied by pair of hydrogen bonds $N5-H5\cdots O6$ and $O4-H4\cdots O5$ are further inter-connected with π -stacking interactions supported by a weak $O3-H5\cdots N5$ hydrogen bond between the nicotinic acid nitrogen atom and the xanthinol hydroxyl group (Fig. 4). As a result, a non-covalent chain of weakly bonded ion pairs is formed along Y-axis. It is noteworthy, that the observed geometry clearly demonstrates the ability of the theophylline fragments to interact with heteroaromatic rings via π -stacking interactions, that can be further supported by a geometrically-matching OH group from side-chain substituent. This type of conjugated interaction can be of great importance in binding modes occurring in biological systems for example with histidine ring.

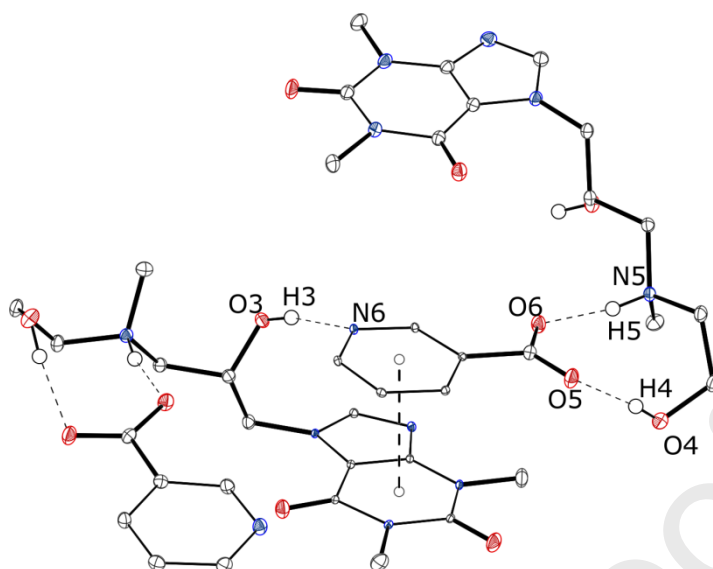


Fig. 4. Schematic representation of the strongest intermolecular interactions constituting crystal structure of (*S*)-(+)-**9**. Non-H-bonding hydrogen atoms have been removed for clarity. Hydrogen bonds donor-acceptor distances and angles: O4-H4 \cdots O5 2.657(4) Å, 171(4) $^\circ$; N5-H5 \cdots O6 2.655(4) Å, 169(4) $^\circ$; O3-H5 \cdots N5 2.784(4) Å, 166(5) $^\circ$; π -stacking marked as a dashed line: the distance between centroids 3.460(2) Å, plane shift: 0.423(5) Å, fold angle: 1.94(14) $^\circ$.

2.5. Determination of the Lipase Stereopreference.

Thanks to the synthesized analytical standard (*R*)-(+)-**4** and its' further utilization as a reference compound during both polarimetric and chromatographic (HPLC) analyses, we could postulate that the stereochemical course of the performed enzymatic reactions is in agreement with Kazlauskas' empirical rule [60] regarding lipases' enantioference towards chiral *sec*-alcohols. This observations correlated well with the results of molecular docking (Fig. 5), which is an excellent tool for studies of enzyme catalysis, i.e. to envision the enantiomeric preference of the enzyme proteins toward small organic molecules. To rationalize the observed enantioselectivity of the (CAL-B)-catalyzed methanolysis of *rac*-**5** an enzyme–substrate molecular docking protocol using non-commercial AutoDock Vina [61] software was applied. In shortening, before docking procedure was performed, the CAL-B crystal structure taken from the Protein Data Bank (PDB), with the code 1TCA [62], was appropriately prepared by removing all nonstandard (non-protein) molecules including *N*-acetyl-D-glucosamine and conserved crystal waters in order to avoid steric clashes within model and by adding polar hydrogen atoms (see Experimental section). As it is the first step of whole catalytic cycle [namely, the attack of serine residue (Ser105) at the carbonyl carbon atom of substrate *rac*-**5**], which primarily determines the enantioselectivity of the reaction according to the well-known mechanism of action of serine hydrolases [63], the two enantiomers of acetic ester of chiral chlorohydrin [(*R*)-(+)-**5** and (*S*)-(–)-**5**] were docked

independently into the active site of target structure of CAL-B enzyme. As a result of this calculations, nine of the most energetically favourable binding modes being the relevant docking poses for the ligand–protein complexes for each substrate molecule **5** were generated, and the results of their binding affinity energies [ΔG_{calc} (kcal/mol)] are shown in Tables S2 and S3 placed in Supporting Information. Next, on the basis of distinguishable sets of docking data and the docking conformational search, we have examined in detail all the unproductive and productive binding poses for both enantiomers' complexes. For clarity, productive poses are defined as a stable conformations compatible with the attack of the catalytic serine to the electrophilic carbon atom of the acyl group, and thus enable the generation of an acyl-enzyme reactive complexes (the so-called catalytic superior conformation). A distance criterion that has to be respected in order to allow the nucleophilic attack of the catalytic serine is around 4.0 Å [64–67]. From this analysis it became clear that only the (*R*)-enantiomer displayed a consistent orientation within the CAL-B binding site to obtain near attack conformations (NACs) leading to catalytically productive complexes [Fig. 5, R (left picture)]. In this regard, for catalytically productive binding, the (*R*)-enantiomer of the substrate molecule positioned its larger substituent (1,3-dimethylxanthine group) towards the hydrophobic surface of CAL-B consisting of Leu140 and Ala141 residues; meanwhile, the aliphatic chain substituent possessing the acyl moiety was oriented toward the catalytic triad without any steric clash with enzyme residues. In this case, for the fast-reacting enantiomer (*R*)-(+)-**5** only two conformations maintained all of the key hydrogen bonds in CAL-B active site, and the most optimal reached the 3.7 Å long distance between the Ser105 residue and the carbonyl function of the (*R*)-acetate suitable for effective nucleophilic attack. Moreover, the N–O distance in the NAC between nitrogen atom of Gln157 and oxygen atom of carbonyl group of the substrate (*R*)-(+)-**5** is 3.3 Å, and H–O distances between hydrogen atom of hydroxyl group of Thr40 and both oxygen atoms of the ester group belonging to (*R*)-(+)-**5** is in the range of 3.0–3.1 Å. As a consequence, if an acyl–enzyme intermediate was formed through a catalytically productive tetrahedral intermediate, it would be obvious that the oxyanion of the (*R*)-enantiomer of racemic substrate (*R*)-(+)-**5** was better stabilized through the key hydrogen bonding network with the oxyanion hole residues (Thr40, Gln106 and Gln157) as well as the catalytic residue (Ser105), respectively.

In contrary, for the slower-reacting enantiomer (*S*)-(–)-**5**, none of the conformations maintained the key hydrogen bonding required for catalysis [Fig. 5, S (right picture)]. Moreover, the distances between the carbonyl atom in the acyl moiety and the oxygen atom of the catalytic serine residue exceed >4.0 Å (see Supporting Information), and thus all

generated conformations of (*S*)-(-)-**5** are catalytically unproductive since it is too far for rapid Ser105 nucleophilic attack to occur. Moreover, the distances required for the stabilization of the acyl-enzyme by the oxyanion hole residues also disfavored catalytic transformation of (*S*)-(-)-**5**.

The other reasons of such a difference in binding orientation between two studied enantiomers of **5** in catalytic cavity of CAL-B can be rationalized by encountered steric clashes of xanthine ring system of (*S*)-(-)-**5** with Leu140 residue of the protein from one side, and by its strong interactions in the stereospecificity acid-binding pocket from the other side. In this regard, especially hydrogen-bonding between one of the carbonyl group's oxygen atom in the 1,3-dimethylxanthine ring and the hydrogen atoms of the OH groups belonging to catalytic Ser105 (2.8 Å) as well as Trp104 (3.1 Å) and Gln157 (3.4 Å) play a fundamental role. Moreover, it is impossible for (*S*)-(-)-**5** to bind in the reactive pose, due to the presence of chlorine atom presented in the aliphatic part of the substrate that would clash with the protein catalytic triad. Additional steric bulk is provided in the active site by His224 what forces xanthine ring to be pointed away from the CAL-B binding site.

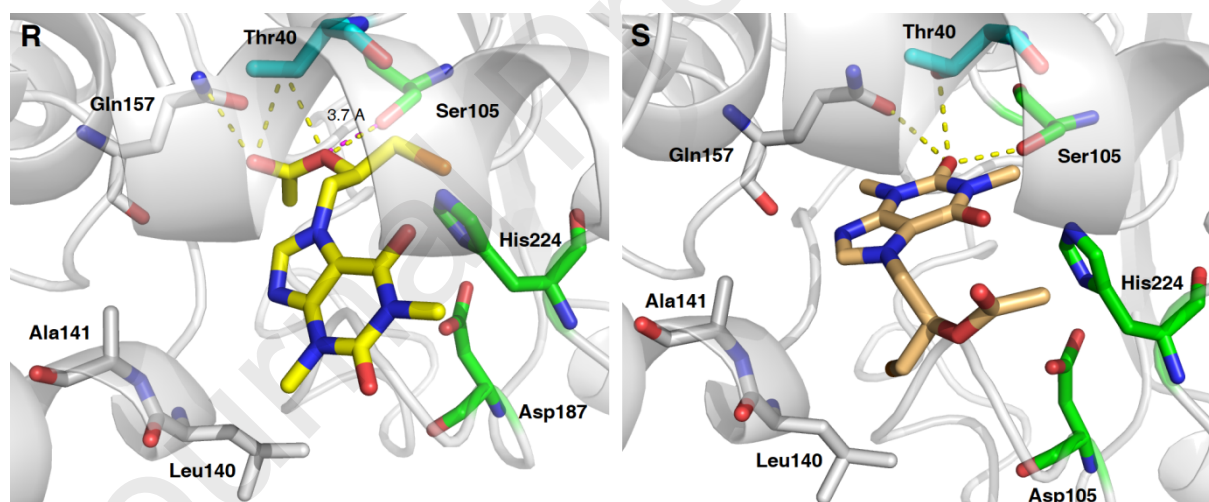


Fig. 5. Predominant conformations of (*R*)-(+)-**5** (yellow sticks) (see R) and (*S*)-(-)-**5** (lightorange sticks) (see S) in CAL-B (PDB ID: 1TCA; shown as gray-colored cartoon diagram) active site. The residues constituting the catalytic triad (Asp187-His224-Ser105) of CAL-B are shown in green sticks representation. The oxyanionic Thr40 residue is shown in cyan. The rest of the most significant residues contributing to the stabilization of *rac*-**5** enantiomers by polar interactions (yellow dashed lines) and by CH-CH van der Waals (vdW) interactions are shown in gray sticks representation. Nitrogen atoms are presented with blue color, the oxygen atoms with red color and the chlorine atoms with orange. The overall enzyme structure is shown as a gray cartoon diagram. The selected mutual distances between the respective amino acid residues, and the ligands' atoms are given in Ångström. The different orientation of the enantiomers toward Ser105 and Thr40 is clearly visible. Only the fast-reacting (*R*)-enantiomer (see R) is near Ser105 (3.7 Å; the distances are indicated by magenta dashed lines) and additionally stabilized through the formation of hydrogen bonds (yellow dashes) with the Thr40 residue (3.0–3.1 Å, not shown for clarity) and Gln157 (3.3 Å, not shown for clarity).

When analyzing all binding mode proposals of the formed complexes between CAL-B and both enantiomers of **5** the low reaction rates as well as low enantioselectivity for the performed EKR of *rac*-**5** could also be rationalized. Two first predominant conformations of the lowest absolute binding free energies [$\Delta G_{\text{calc}} = -6.3$ (kcal/mol) for (*R*)-(+)-**5** and $\Delta G_{\text{calc}} = -6.5$ (kcal/mol) for (*S*)-(–)-**5**, see Supporting Information] show that enantiomers of the employed ligand **5** molecule are situated preferably in another, common for them both, unproductive poses (Fig. 6). In this case, the alkyl side chain with the acyl moiety of **5** is pulled far away from the catalytic triad and the oxyanion hole, thus sterically accommodating in the pocket surrounded by Leu140, Ala141, and Gln157 residues where is less constrained.

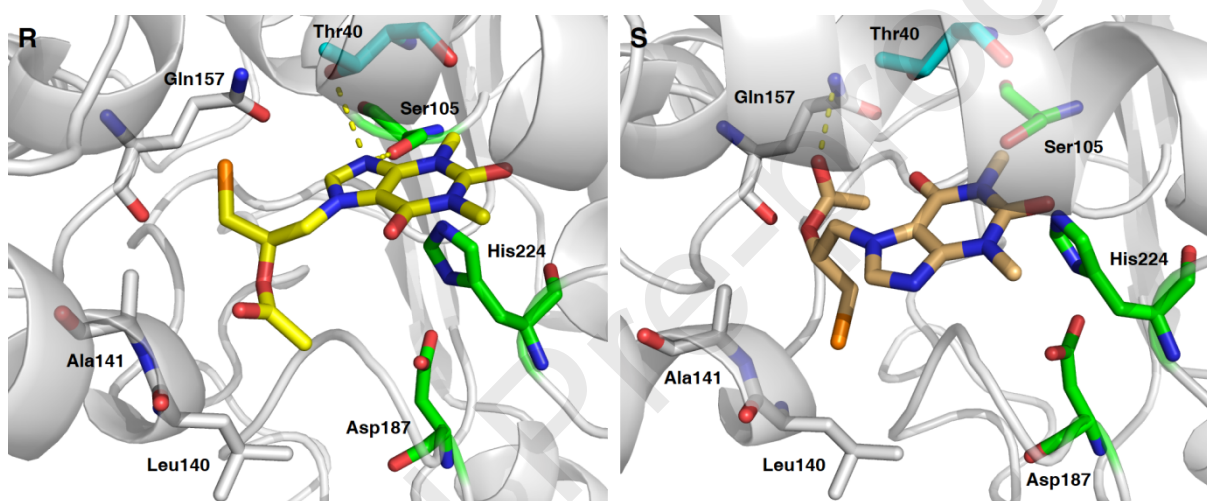


Fig. 6. Binding mode proposals for the lowest binding potential energy complexes of CAL-B (PDB ID: 1TCA, shown as gray-colored cartoon diagram) active-site with (*R*)-(+)-**5** (yellow sticks) (see R) and (*S*)-(–)-**5** (lightorange sticks) (see S). The formation of intermolecular hydrogen bonds is represented by yellow dashes.

In the case of (*R*)-(+)-**5** it was the double H-bonding between nitrogen atom of the xanthine ring and both the hydroxyl groups present in Ser105 (3.1 Å) and Thr40 (3.2 Å) as well as CH–CH van der Waals (vdW) interactions between alkyl side-chain of **5** and hydrophobic aminoacid residues (Ala141, Gln157 and Ile189) that play an important role in stabilizing the lowest energy complex of ‘uncatalytical accommodation’ [Fig. 6, R (left picture)]. Entangling the relevant conserved serine residue in the hydrogen-bonding with imidazolic N-atom of xanthine moiety additionally cease its nucleophilic potential toward the carbonyl group of the acyl compound **5**. In turn, the highest ligand-binding affinity mode for (*S*)-(–)-**5** revealed that unproductive conformation with impede access to the carbonyl group is stabilized by steric clashes of the xanthine ring with catalytic triad residues, CH–CH interactions with hydrophobic residues that surround active site, and strong 3.1 Å long

intermolecular hydrogen bonding between oxygen atom of carbonyl group present in the substrate's acyl moiety and the amide side chain of Gln157 [Fig. 6, S (right picture)]. Here, it is important to mention that in each case the aliphatic side chain of **5** bearing a terminal electron-dense chlorine atom is out into the hydrophobic cavity, thus preventing successful delivery of the reactive ester group near to the activated Ser105 residue.

Docking results clarified that low enantioselectivity and activity of CAL-B toward *rac*-**5** is mainly due to inaccessibility of the substrate **5** enantiomers to the catalytic machinery. This is due to predominance of the unproductive orientations of both the enantiomers of **5** in the hypothetical complexes with CAL-B. On the other hand, the proposal of "NACs-type effect" calculated by molecular docking protocol indicates only hypothetical orientations of **5** enantiomers in the enzyme active site – the proximity of their ester groups toward both the catalytic and oxyanion hole residues as well as the main conformations of the substrate's xanthine ring within the cavity. Although NACs model contributes in some extent to the entire catalytic effect, it does not fully address the origin of the catalytic behavior of the CAL-B in chiral recognition of enantiomers since it only predicts substrate-enzyme binding states (binding affinity) and not the tetrahedral intermediates of the acylation step. Therefore, in order to verify the validity of the NACs model used in this study it would be worth to supplement molecular docking with the calculations of free-energy ($-\Delta\Delta G$) between two transition states (TS) derived from each of the potentially formed tetrahedral CAL-B-enantiomer (**5**) intermediates, respectively. Unambiguously, the identification of the rate-limiting acyl-enzyme TS (or the first tetrahedral intermediate) performed *via* molecular modeling (MM) [68–74] and/or hybrid quantum mechanical/molecular mechanical (QM/MM) molecular dynamics (MD) simulations [75–79] and/or so-called 'substrate-imprinted docking' (covalent docking) [78,79] could further supports the current calculations and strengthen molecular insights of the CAL-B catalytic behavior in distinguishing between enantiomers of chiral xanthine esters in enantioselective deacetylations.

2.6. Determination of optical purity of titled APIs.

According to world regulatory authorities [i.e. U.S. Food and Drug Administration (FDA) and European Medicines Agency (EMA)] that tightly control human clinical trials of drug candidates, one of the absolutely necessary task is the determination of the optical purity of APIs with chiral properties before their commercialization and administration. This restriction mainly stems from catastrophic failures of the pharmaceutical industry (i.e. the tragic birth

defects from thalidomide, ‘*the thalidomide tragedy*’), which taught scientific community that even negligible enantiomeric impurities may pose a significant danger for human health and life. Fortunately, in the case of diprophylline (**7**) and xanthinol (**8**) both their enantiomers constitute lack of therapeutic-risk-management for patients. Nevertheless, separation of stereoisomers of the above-mentioned methylxanthines with the highest possible efficiency, and furthermore, estimation of their single enantiomers’ affinity toward different receptors within which they interact in the cells [i.e. adenosine receptors, phosphodiesterases (PDEs), prostaglandin E synthase, xanthine oxidase etc.] seems to be reasonable from the viewpoint of eudismic ratios evaluation and clinical effectiveness.

The investigation of enantiomeric excess (% ee) of non-racemic diprophylline (**7**) was rather easy task to perform since it has been already reported by Brandel et al. [38] that the baseline resolution for (*R*)- and (*S*)-enantiomers of **7** under *c*-HPLC analyses can be achieved on a Chiralpak IC column (Daicel group, Chiral Technologies Europe) by eluting the samples at 25 °C with the mobile phase composed of heptane/EtOH (70:30, v:v) mixture with the flow-rate of 1.0 mL/min and applying the wavelength for UV detection set at 273 nm. Under very similar HPLC conditions (heptane was replaced by *n*-hexane), but using different chiral column [Lux i-Cellulose-5 (Phenomenex, US)], we managed to obtain full analytic separation of the very well-shaped peaks of *rac*-**7** with retention times of 38.85 min for (*R*)-enantiomer and 44.45 min for (*S*)-enantiomer, respectively (see Supporting Information). Although the time of the analyses were over two-fold longer when compared to the method designed by Brandel and co-workers using Chiralpak IC column, we felt extremely satisfied with alternative chiral stationary phase [cellulose tris(3,5-dichlorophenylcarbamate) loaded in Lux i-Cellulose-5 column.

The next task was to estimate enantiomeric purity for the samples of non-racemic xanthinol (**8**). This time, the assignment turned to be more complex than for afore-mentioned diprophylline (**7**). At first, we decided to follow the method established by Grace and co-workers [40], who reported successful enantiomeric excess assessment of optically active xanthinol (**8**) using standard NMR analyses employing commercially available (*S*)-(+)-1-(9-anthryl)-2,2,2-trifluoroethanol [(*S*)-(+)-**10**] as the chiral solvating agent (CSA). However, to our disappointment authors of this publication did not provide any details concerning the conditions used for the performed spectral analyses (i.e. type of the deuterated solvent, amounts of the used CSA etc.) as well as the final results (analytical data, spectra copies etc.). Nevertheless, when taking into account that for the chiral separations of CSA-mediated NMR methodology non-equivalence interactions (especially hydrogen bonding) between

enantiomers of the examined compound and CSA agent are prevalent for the formation of the appropriate diastereomeric complexes, which guarantee a proton resonance signal differentiation, therefore, all of the ^1H NMR measurements were intentionally performed in one of the apolar and aprotic solvent. At first, we decided to record the spectra in fully deuterated benzene (C_6D_6) at 25 °C using standard acquisition parameters (see Experimental). After the first set of experiments, the results obtained were fully satisfactory, and thus the influence of the solvent nature on the magnitude of the observed non-equivalence interactions between enantiomers was deliberately omitted. Then, the variation of ^1H chemical shift increments ($\Delta\delta_{\text{H}}$) for racemic xanthinol (*rac*-**8**) in the presence of various molar excess of (*S*)-(+)-**10** was examined and the results are shown in Fig. 7. Typical chiral discrimination experiments were conducted as follows. The ^1H NMR spectra of *rac*-**8** with gradually increased amount of (*S*)-(+)-**10** as CSA were recorded in C_6D_6 solution. The first spectrum was obtained without CSA (Fig. 7, violet spectrum), then sequential portions of (*S*)-(+)-**10** (1 equiv) were added, and the respective signals were integrated after each addition. As can be seen, the addition of just 1 equiv of (*S*)-(+)-**10** to the solution of *rac*-**8** in benzene- d_6 was almost sufficient for the appropriate signal splitting, and thus complete separation of the two enantiomers of xanthinol (**8**) could be obtained (Fig. 7, green spectrum). In this context, the hydrogen resonance of the methyl groups directly attached to xanthine ring system (H_1 , H_2) as well as to N-atom of amine moiety (H_7), which normally appear as the singlets, now in the presence of CSA turned into doublets. However, better peak separation was required for reliable integration, and therefore subsequent portions of (*S*)-(+)-**10** were added in an effort to improve the baseline resolution. The accurate molar ratio of (*S*)-(+)-**10**/*rac*-**8** leading to full separation of the peaks deriving from different methyl protons' signals in the NMR spectrum turned out to be 2:1 (Fig. 7, blue spectrum). Especially the protons (H_1) belonging to one of the methyl group present in the xanthine ring (Fig. 7, highlighted with purple frame) were not only very well-separated, but also situated on the ^1H NMR spectra far from the other potentially interfering signals, that are: (i) multiplet of methylene group of the ethanoloamine side-chain and (ii) doublet of doublets corresponding to diastereotopic protons of the methylene group located nearby asymmetric carbon atom and nitrogen atom which belongs to xanthine moiety. This enabled that their peak-area ratios were approximately 1:1 as expected.

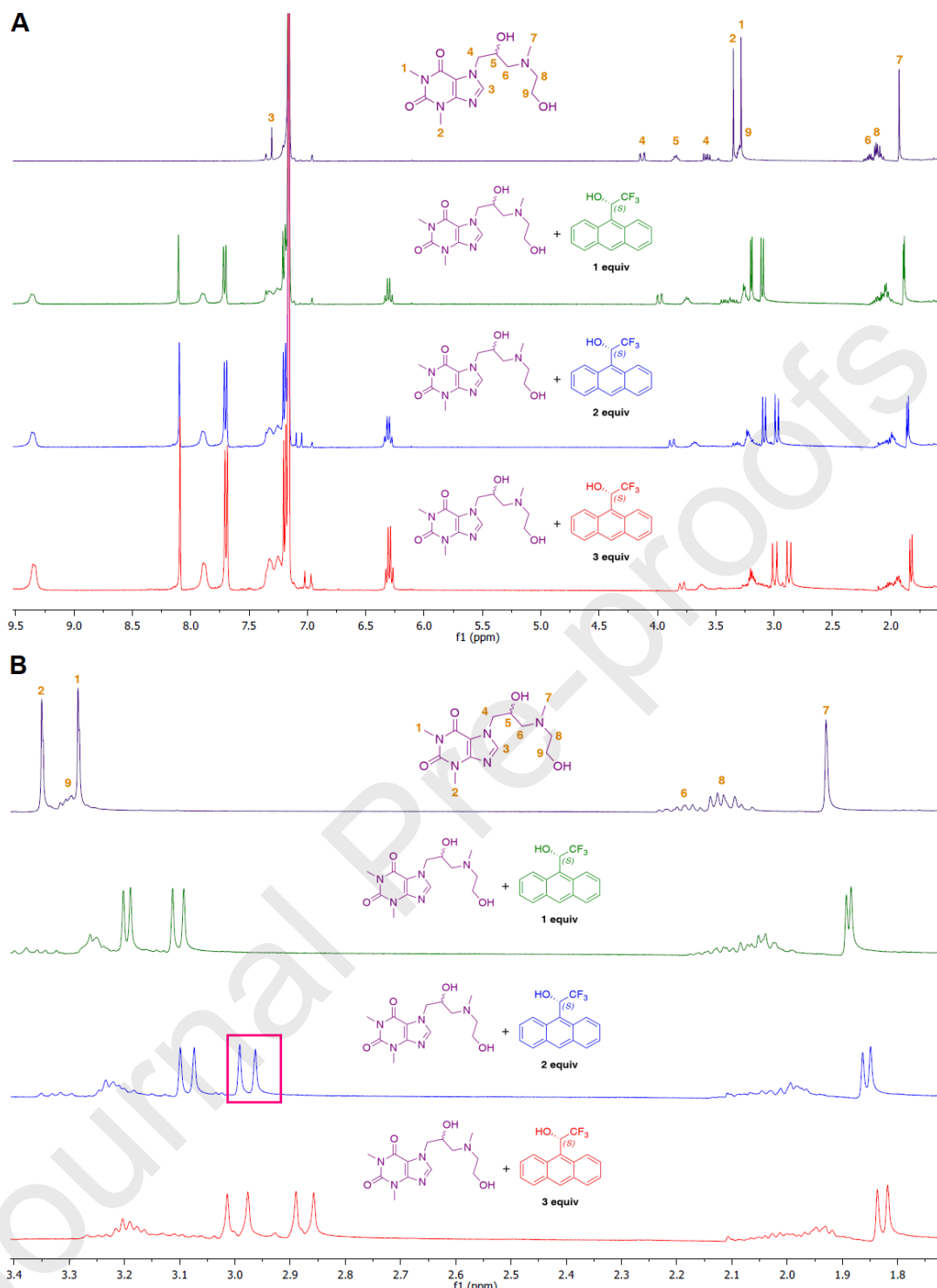


Fig. 7. Chiral discrimination of the methyl group protons (H_1 , H_2 and H_7) in the ^1H NMR spectrum of racemic xanthinol (*rac*-**8**) (violet) in the presence of 1-fold (green), 2-fold (blue) and 3-fold (red) molar excess of (*S*)-(+)-1-(9-anthryl)-2,2,2-trifluoroethanol (>98% ee) [(*S*)-(+)-**10**] in deuterated benzene (C_6D_6) recorded at 400 MHz, respectively. (A) Whole ^1H NMR spectrum and (B) the expansion of ^1H NMR spectrum for the aliphatic region (high-field range; 1.7–3.4 ppm).

Next, the afore-optimized method was extended toward the samples of non-racemic xanthinol [(*S*)-(+)-**8**]. The expansions of optimized spectra are depicted in Fig. 8. Hopefully, the application of a 2-fold molar excess of (*S*)-(+)-**10** resulted in determination of the

enantiomeric composition of (*S*)-(+)-**8**, however, the results obtained from the integration of the ¹H NMR signals for each enantiomeric mixture of optically active xanthinol [(*S*)-(+)-**8**] unmatched with the results of the performed synthetic transformations (see Scheme 1 and Scheme 3). For example, the assessed by NMR values of the % ee's for (*S*)-(+)-**8** derived from classical chemical route (Fig. 8, red coloured fragment of the spectra, B) was 95% and for (*S*)-(+)-**8** obtained from enzymatic route (Fig. 8, purple coloured fragment of the spectra, C) was 81%, respectively. As can be seen, it is obviously not possible to achieve such highly enantiomerically enriched xanthinol (**8**) from starting materials with significantly lower ee-values. For reminder, the epoxide (*R*)-(+)-**3** synthesized from the kinetically-resolved chlorohydrine (*R*)-(+)-**4** using lipases was characterized by enantioenrichment at 71% ee level (see Scheme 1), and the one used in classical chemical route reached 92% ee (see Scheme 3) according to *c*-HPLC indications. Based on these experiments it was clear that assignment of the optical purity of non-racemic xanthinol [(*S*)-(+)-**8**] samples *via* CSA-mediated NMR method might be burdened with the risk of a large error. We suppose that this could be due to overlapping of the neighboring signals with the peak that corresponds to (*S*)-enantiomer of the examined API **8**, and thus inflate the value of its integral. Another sensible explanation for this phenomenon is that other traces of impurities present in the samples affected the result of the analytical experiment.

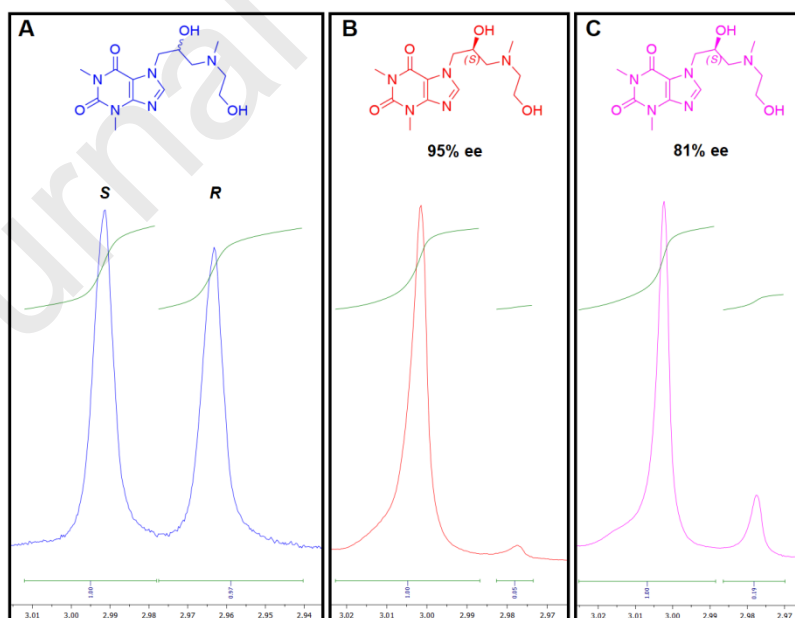


Fig. 8. Expansions of ¹H NMR spectra [aliphatic (up-field) region in C₆D₆ solution] of racemic xanthinol (*rac*-**8**) (blue, A), enantioenriched xanthinol [(*S*)-(+)-**8**] obtained from classical chemical route (red, B), and obtained from enzymatic route (purple, C) complexed with 2 equiv of (*S*)-(+)-1-(9-anthryl)-2,2,2-trifluoroethanol (>98% ee) [(*S*)-(+)-**10**], respectively.

Since other NMR chiral reagent, namely (*S*)-(-)-1,1'-bi(2-naphthol) [(*S*)-(-)-BINOL, **11**], is amply demonstrated by literature reports [80–86] to be very efficient in discriminating between enantiomers in solution, we decided to adopt it in order to determine the enantiopurity of (*S*)-(+)-**8**. The experimental sequence was exactly the same as for (*S*)-(+)-**10**. The formation of two diastereomeric host–guest complexes coexisting in the solution gave the best resolution for the signals of H₁ protons resulting in doublet (H_{1A} and H_{1B}) with 3 equiv of (*S*)-(-)-BINOL, however, they overlapped with the adjacent singlet corresponding to the H₂ protons (Fig. 9, red spectrum). The addition of 1 molar equiv more of the atropisomeric CSA **11** resulted in a similarly distinct signal separation, however the reliability of the interpretations still suffered from presence of H₂ protons signals (not shown herein). In conclusion, although the NMR techniques provided a rapid and solvent consumption-free analyses, an efficient enantioseparation for the xanthinol (*rac*-**8**) was not obtained due to overlapping of the neighboring signals.

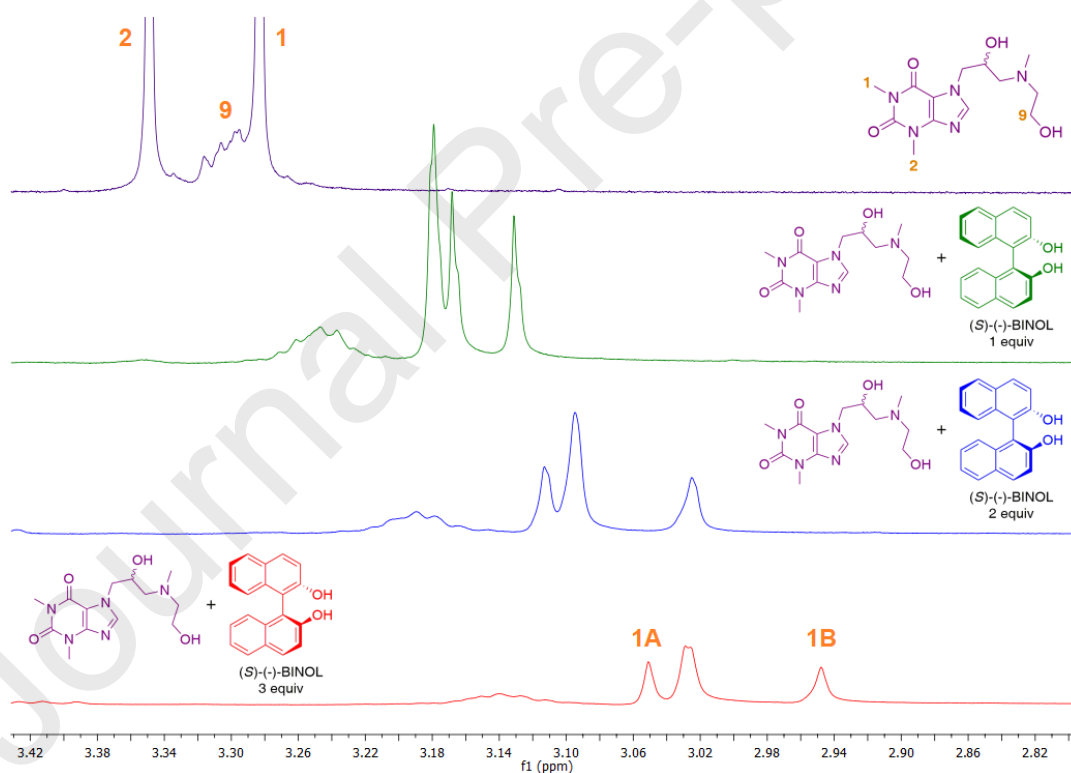


Fig. 9. Chiral discrimination of the methyl group protons (H₁) in the ¹H NMR spectrum of racemic xanthinol (*rac*-**8**) (violet) in the presence of 1-fold (green), 2-fold (blue) and 3-fold (red) molar excess of (*S*)-(-)-1,1'-bi(2-naphthol) (99% ee) [(*S*)-(-)-BINOL, **11**] in deuterated benzene (C₆D₆) recorded at 400 MHz, respectively. The figure shows the extension of ¹H NMR spectrum for the aliphatic region (high-field range).

Thereafter, we directed our efforts towards developing an analytical method that would be more reliable in terms of optical purity evaluations. The natural choice fell on *c*-

HPLC since it allows to determine enantiomeric impurity in the range below 0.1%, which is required by major pharmacopeias. We screened sample of racemic xanthinol (*rac*-**8**) in three mobile phase conditions: normal, reverse, and polar organic by using seven different Lux phase columns for each HPLC system. The best results were obtained with a Lux i-Cellulose-5 column (250 mm × 4.6 mm, 5 μm particle size) in normal phase mode consisted of [*n*-hexane/EtOH/DEA (70:30:0.1, v/v); at flow-rate = 1.0 mL/min; λ = 280 nm; 26 °C] (Fig. 10, A) and polar organic elution conditions [MeOH/2-PrOH/DEA (90:10:0.1, v/v); at flow-rate = 1.0 mL/min; λ = 280 nm; 26 °C]; where DEA stands for diethylamine (Fig. 10, B).

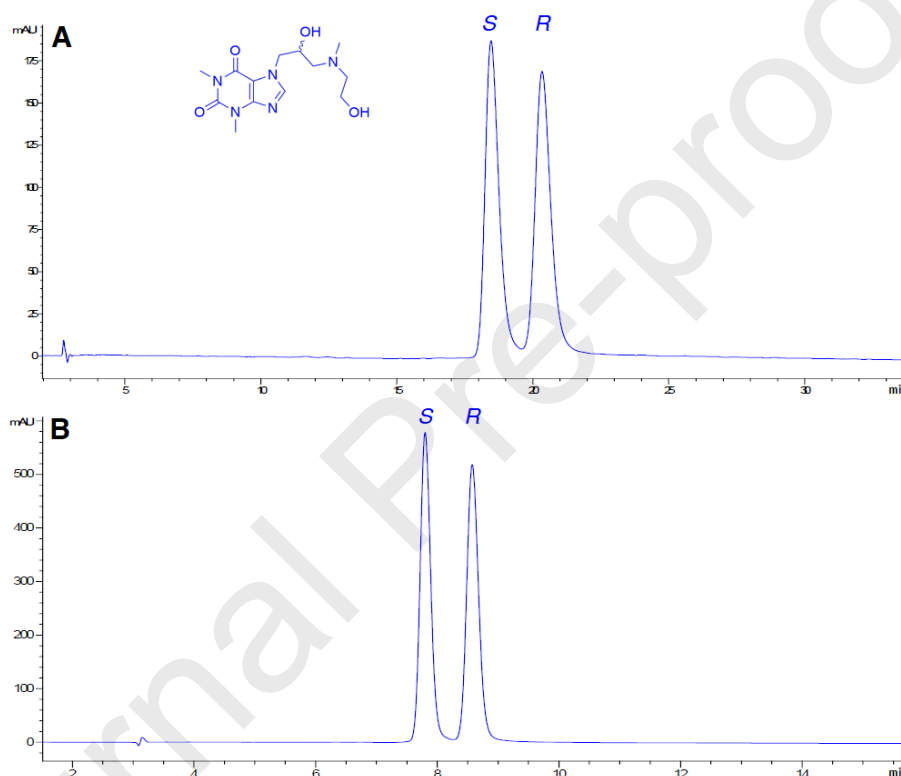


Fig. 10. The HPLC chromatograms of racemic xanthinol (*rac*-**8**) performed in: normal-phase mode (A) and in polar-organic phase mode (B). Chiral phase HPLC analysis of *rac*-**8** gave the respective retention times (t_R) of (*S*)-(+)-**8** and (*R*)-(-)-**8**: 18.521 and 20.534 (A) and 7.819 and 8.651 (B) minutes, respectively.

Both the developed conditions gave superb results in terms of baseline resolution thanks to which the chromatograms of this sample displayed two peaks of equal areas. Moreover, time of analysis were also optimal (ca. 22 min for normal phase conditions and ca. 9 min for polar organic phase conditions). However, slightly better chiral resolutions were attained in the case of polar organic mobile phase conditions as the resolution factor (R_s) reached a value of 2.32 and selectivity factor (α) that was 1.10. In turn, HPLC analysis with normal phase elution system gave $R_s = 1.89$ and $\alpha = 1.10$, respectively. The developed methods were repeated for the respective samples of optically active xanthinol [(*S*)-(+)-**8**],

affording this time desired API with 65% ee from enzymatic route and 89% ee from conventional synthetic pathway. It is worth noting that when using HPLC in normal-phase mode the enantiomeric excess for (*S*)-(+)-**8** obtained *via* convenient chemical route was slightly over-valued as it was established to be 91% ee (see Supporting Information). Therefore, we realized that chiral phase HPLC analysis performed in a polar-organic phase mode is more reliable in this case.

CONCLUSIONS

The present study reports on the first example of the chemoenzymatic syntheses of optically active title pharmaceutically-valuable xanthine derivatives [(*R*)-(-)-**7**, (*S*)-(+)-**8** and (*S*)-(+)-**9**], which have been explored by using classical enzymatic kinetic resolution methodology toward their common chlorohydrin acetate precursor *rac*-**5**. A set of commercially available lipase preparations were screened and extensively manipulated in either the esterification or hydrolytic mode for the enantioselective KR protocol of the respective racemates *rac*-**4–6** in organic solvents. We failed in enantioselective transesterification attempt to resolve enantiomers of chlorohydrin *rac*-**4**, which was likely due to the very low solubility of that compound in suitable organic solvents. The key point of the synthesis was the switch of the method on kinetically-controlled enantioselective methanolysis of chlorohydrin acetate *rac*-**5** catalyzed by immobilized *Candida antarctica* lipase type B (Novozym 435). An efficient enantioseparation furnishing both resolution products with acceptable high enantioselectivity ($E > 10$) and enantiomeric excesses (in the range of 65–77%) were accomplished with the biocatalytic system composed of Novozym 435 and 10 equiv of MeOH in CH₃CN or 1,4-dioxane as co-solvents. Lipase-catalyzed stereochemical discrimination of *rac*-**5** enantiomers was successfully scaled up to a 500-mg of racemic substrate thus affording both EKR products (*R*)-(+)-**4** and (*S*)-(-)-**4** with slightly improved 71–78% ee and $E = 14$. Moreover, docking evaluations concerning absolute binding free energy calculations for both substrate's enantiomers [(*R*)-(+)-**5** and (*S*)-(-)-**5**] and CAL-B protein molecule was performed. *In silico* prediction of binding selectivity showed excellent agreement with experimental data that (*R*)-enantiomer of *rac*-**5** fits better into the active site of CAL-B than its counterpart, and is therefore converted at a higher rate. Nevertheless, low enantioselectivity of CAL-B might be explained by the fact that both enantiomers are incapable to obtain near attack conformations in the active site. By this, we have demonstrated that enantiomeric preference of CAL-B toward xanthine derivative can be evaluated using simple non-commercial computational

methodology; however, fully proper elucidation of the enzyme chiral recognition toward optical isomers studied herein definitely requires additional molecular modelling simulations of tetrahedral intermediates to calculate the free energy difference ($-\Delta\Delta G$) between two transition states of the respective CAL-B-**5** complexes. An understanding of these details is essential for rational re-design of enantioselective enzyme-catalyzed transformations of chiral xanthenes. Despite the achieved moderate results of both enantiomeric APIs in terms of optical purity (57–65% ee), the new chemoenzymatic route as well as all crucial analytical aspects, including HPLC baseline separations of the respective racemates and XRD crystal structures of both examined pharmaceuticals will be of great importance with respect to future biocatalytical investigations on these drugs.

Declaration of Competing Interest

There is no conflict of interest.

Acknowledgements

This research was financially supported by the National Science Centre (NCN) of Poland in the framework of grant SONATA 15 (No: 2019/35/D/ST4/01556). The Warsaw University of Technology, Faculty of Chemistry is appreciated (statute work). The authors wish to gratefully acknowledge Prof. Jan Plenkiewicz for proof-reading as well as critical opinions helpful for preparing this manuscript and Dr Zbigniew Ochal who recruited M.M. for volunteering internship. We would also like to express our special gratitude to Phenomenex (Torrance, CA) for helping us in determination of HPLC chiral separation conditions performed for racemic xanthinol within framework of their free chiral screening project (PhenoLogix).

Authorship contribution statement

Pawel Borowiecki: Conceptualization, Methodology, Validation, Investigation, Formal synthesis and analysis, Molecular Docking Studies, Data curation, Writing – original draft, Writing – review & editing & revision, Funding acquisition, Supervision. **Mateusz Mlynek:** Investigation (assistance during synthesis and analysis). **Maciej Dranka:** Investigation (XRD analyses).

Appendix A. Supplementary material

Experimental details and characterization of products are given in Supporting Information. Supplementary data to this article can be found online at <https://doi.org/XXX>.

References

- [1] B.B. Fredholm (Ed.) Methylxanthines, Handbook of Experimental Pharmacology Vol. 200 Springer-Verlag Berlin Heidelberg 2011.
- [2] E. Szymańska, A. Drabczyńska, T. Karcz, C.E. Müller, M. Köse, J. Karolak-Wojciechowska, A. Fruzinski, J. Schabikowski, A. Doroz-Płonka, J. Handzlik, K. Kieć-Kononowicz, Similarities and differences in affinity and binding modes of tricyclic pyrimido- and pyrazinoxanthines at human and rat adenosine receptors, *Bioorg. Med. Chem.* 24 (18) (2016) 4347–4362.
- [3] M.M. Van der Walt, G. Terre'Blanche, 1,3,7-Triethyl-substituted xanthines--possess nanomolar affinity for the adenosine A1 receptor, *Bioorg. Med. Chem.* 23 (20) (2015) 6641–6649.
- [4] A.R. Beaglehole, S.P. Baker, P.J. Scammells, Fluorosulfonyl-substituted xanthines as selective irreversible antagonists for the A(1)-adenosine receptor, *J. Med. Chem.* 43 (26) (2000) 4973–4980.
- [5] J.R. Pfister, L. Belardinelli, G. Lee, R.T. Lum, P. Milner, W.C. Stanley, J. Linden, S.P. Baker, G. Schreiner, Synthesis and biological evaluation of the enantiomers of the potent and selective A1-adenosine antagonist 1,3-dipropyl-8-[2-(5,6-epoxynorbornyl)]-xanthine, *J. Med. Chem.* 40 (12) (1997) 1773–1778.
- [6] M.M. van der Walt, G. Terre'Blanche, Selected C8 two-chain linkers enhance the adenosine A1/A2A receptor affinity and selectivity of caffeine, *Eur. J. Med. Chem.* 125 (2017) 652–656.
- [7] R. Yadav, R. Bansal, S. Kachler, K.N. Klotz, Novel 8-(p-substituted-phenyl/benzyl)xanthines with selectivity for the A2A adenosine receptor possess bronchospasmolytic activity, *Eur. J. Med. Chem.* 75 (2014) 327–335.
- [8] M.M. Van der Walt, G. Terre'Blanche, A. Petzer, A.C. Lourens, J.P. Petzer, The adenosine A(2A) antagonistic properties of selected C8-substituted xanthines, *Bioorg. Chem.* 49 (2013) 49–58.
- [9] A. Drabczyńska, O. Yuzlenko, M. Köse, M. Paskaleva, A.C. Schiedel, J. Karolak-Wojciechowska, J. Handzlik, T. Karcz, K. Kuder, C.E. Müller, K. Kieć-Kononowicz,

- Synthesis and biological activity of tricyclic cycloalkylimidazo-, pyrimido- and diazepinopurinediones, *Eur. J. Med. Chem.* 46 (9) (2011) 3590–3607.
- [10] R. Sauer, J. Maurinsh, U. Reith, F. Fülle, K.N. Klotz, C.E. Müller, Water-soluble phosphate prodrugs of 1-propargyl-8-styrylxanthine derivatives, A(2A)-selective adenosine receptor antagonists, *J. Med. Chem.* 43 (3) (2000) 440–448.
- [11] P.G. Baraldi, S. Baraldi, G. Saponaro, D. Preti, R. Romagnoli, L. Piccagli, A. Cavalli, M. Recanatini, A.R. Moorman, A.N. Zaid, K. Varani, P.A. Borea, M.A. Tabrizi, Novel 1,3-dipropyl-8-(3-benzimidazol-2-yl-methoxy-1-methylpyrazol-5-yl)xanthines as potent and selective A(2)B adenosine receptor antagonists, *J. Med. Chem.* 55 (2) (2012) 797–811.
- [12] J. Hierrezuelo, J. Manuel López-Romero, R. Rico, J. Brea, M. Isabel Loza, C. Cai, M. Algarra, Synthesis of theophylline derivatives and study of their activity as antagonists at adenosine receptors, *Bioorg. Med. Chem.* 18 (6) (2010) 2081–2088.
- [13] T. Borrmann, S. Hinz, D.C. Bertarelli, W. Li, N.C. Florin, A.B. Scheiff, C.E. Müller, 1-alkyl-8-(piperazine-1-sulfonyl)phenylxanthines: development and characterization of adenosine A2B receptor antagonists and a new radioligand with subnanomolar affinity and subtype specificity, *J. Med. Chem.* 52 (13) (2009) 3994–4006.
- [14] M.C. Balo, J. Brea, O. Caamaño, F. Fernández, X. García-Mera, C. López, M.I. Loza, M.I. Nieto, J.E. Rodríguez-Borges, Synthesis and pharmacological evaluation of novel 1- and 8-substituted-3-furfuryl xanthines as adenosine receptor antagonists, *Bioorg. Med. Chem.* 17 (18) (2009) 6755–6760.
- [15] R.V. Kalla, E. Elzein, T. Perry, X. Li, A. Gimbel, M. Yang, D. Zeng, J. Zablocki, Selective, high affinity A(2B) adenosine receptor antagonists: N-1 monosubstituted 8-(pyrazol-4-yl)xanthines, *Bioorg. Med. Chem. Lett.* 18 (4) (2008) 1397–1401.
- [16] J. Zablocki, R. Kalla, T. Perry, V. Palle, V. Varkhedkar, D. Xiao, A. Piscopio, T. Maa, A. Gimbel, J. Hao, N. Chu, K. Leung, D. Zeng, The discovery of a selective, high affinity A(2B) adenosine receptor antagonist for the potential treatment of asthma, *Bioorg. Med. Chem. Lett.* 15 (3) (2005) 609–612.
- [17] P.G. Baraldi, M.A. Tabrizi, D. Preti, A. Bovero, F. Fruttarolo, R. Romagnoli, A.R. Moorman, S. Gessi, S. Merighi, K. Varani, P.A. Borea, [3H]-MRE 2029-F20, a selective antagonist radioligand for the human A2B adenosine receptors, *Bioorg. Med. Chem. Lett.* 14 (13) (2004) 3607–3610.
- [18] P.G. Baraldi, M.A. Tabrizi, D. Preti, A. Bovero, R. Romagnoli, F. Fruttarolo, N.A. Zaid, A.R. Moorman, K. Varani, S. Gessi, S. Merighi, P.A. Borea, Design, synthesis, and biological evaluation of new 8-heterocyclic xanthine derivatives as highly potent and

- selective human A2B adenosine receptor antagonists, *J. Med. Chem.* 47 (6) (2004) 1434–1447.
- [19] A.M. Hayallah, J. Sandoval-Ramírez, U. Reith, U. Schobert, B. Preiss, B. Schumacher, J.W. Daly, C.E. Müller, 1,8-disubstituted xanthine derivatives: synthesis of potent A2B-selective adenosine receptor antagonists, *J. Med. Chem.* 45 (7) (2002) 1500–1510.
- [20] Y.C. Kim, X. Ji, N. Melman, J. Linden, K.A. Jacobson, Anilide derivatives of an 8-phenylxanthine carboxylic congener are highly potent and selective antagonists at human A(2B) adenosine receptors, *J. Med. Chem.* 43 (6) (2000) 1165–1172.
- [21] L. Xia, W.A.C. Burger, J.P.D. van Veldhoven, B.J. Kuiper, T.T. van Duijl, E.B. Lenselink, E. Paasman, L.H. Heitman, I.J. AP, Structure-Affinity Relationships and Structure-Kinetics Relationships of Pyrido[2,1-f]purine-2,4-dione Derivatives as Human Adenosine A3 Receptor Antagonists, *J. Med. Chem.* 60 (17) (2017) 7555–7568.
- [22] P.G. Baraldi, D. Preti, M.A. Tabrizi, F. Fruttarolo, R. Romagnoli, N.A. Zaid, A.R. Moorman, S. Merighi, K. Varani, P.A. Borea, New pyrrolo[2,1-f]purine-2,4-dione and imidazo[2,1-f]purine-2,4-dione derivatives as potent and selective human A3 adenosine receptor antagonists, *J. Med. Chem.* 48 (14) (2005) 4697–4701.
- [23] N.J. Arnold, R. Arnold, D. Beer, G. Bhalay, S.P. Collingwood, S. Craig, N. Devereux, M. Dodds, A.R. Dunstan, R.A. Fairhurst, D. Farr, J.D. Fullerton, A. Glen, S. Gomez, S. Haberthuer, J.D. Hatto, C. Howes, D. Jones, T.H. Keller, B. Leuenberger, H.E. Moser, I. Muller, R. Naef, P.A. Nicklin, D.A. Sandham, K.L. Turner, M.F. Tweed, S.J. Watson, M. Zurini, Potent and selective xanthine-based inhibitors of phosphodiesterase 5, *Bioorg. Med. Chem. Lett.* 17 (8) (2007) 2376–2379.
- [24] T. Mohamed, W. Osman, G. Tin, P.P. Rao, Selective inhibition of human acetylcholinesterase by xanthine derivatives: in vitro inhibition and molecular modeling investigations, *Bioorg. Med. Chem. Lett.* 23 (15) (2013) 4336–4341.
- [25] A. Brunschweiler, P. Koch, M. Schlenk, M. Rafehi, H. Radjainia, P. Küppers, S. Hinz, F. Pineda, M. Wiese, J. Hockemeyer, J. Heer, F. Denonne, C.E. Muller, 8-Substituted 1,3-dimethyltetrahydropyrazino[2,1-f]purinediones: Water-soluble adenosine receptor antagonists and monoamine oxidase B inhibitors, *Bioorg. Med. Chem.* 24 (21) (2016) 5462–5480.
- [26] S. Carradori, R. Silvestri, New Frontiers in Selective Human MAO-B Inhibitors, *J. Med. Chem.* 58 (17) (2015) 6717–6732.
- [27] D.A. Pissarnitski, Z. Zhao, D. Cole, W.L. Wu, M. Domalski, J.W. Clader, G. Scapin, J. Voigt, A. Soriano, T. Kelly, M.A. Powles, Z. Yao, D.A. Burnett, Scaffold-hopping from

- xanthines to tricyclic guanines: A case study of dipeptidyl peptidase 4 (DPP4) inhibitors, *Bioorg. Med. Chem.* 24 (21) (2016) 5534–5545.
- [28] W. Czechtizky, J. Dedio, B. Desai, K. Dixon, E. Farrant, Q. Feng, T. Morgan, D.M. Parry, M.K. Ramjee, C.N. Selway, T. Schmidt, G.J. Tarver, A.G. Wright, Integrated Synthesis and Testing of Substituted Xanthine Based DPP4 Inhibitors: Application to Drug Discovery, *ACS Med. Chem. Lett.* 4 (8) (2013) 768–772.
- [29] M. Eckhardt, E. Langkopf, M. Mark, M. Tadayyon, L. Thomas, H. Nar, W. Pfrengle, B. Guth, R. Lotz, P. Sieger, H. Fuchs, F. Himmelsbach, 8-(3-(R)-aminopiperidin-1-yl)-7-but-2-ynyl-3-methyl-1-(4-methyl-quinazolin-2-ylmethyl)-3,7-dihydropurine-2,6-dione (BI 1356), a highly potent, selective, long-acting, and orally bioavailable DPP-4 inhibitor for the treatment of type 2 diabetes, *J. Med. Chem.* 50 (26) (2007) 6450–6453.
- [30] B.J. Dezube, A.B. Pardee, R.M. Ruprecht, W.J. Novick, Use of xanthines for the preparation of a medicament effective for inhibiting the replication of human retroviruses, EP0484785 A2, 1992.
- [31] S.M. Rida, F.A. Ashour, S.A. El-Hawash, M.M. El-Semary, M.H. Badr, Synthesis of some novel substituted purine derivatives as potential anticancer, anti-HIV-1 and antimicrobial agents, *Archiv. Pharm.* 340 (4) (2007) 185–194.
- [32] A.K. Hayallah, A.A. Talhouni, A.A. Alim, Design and synthesis of new 8-anilide theophylline derivatives as bronchodilators and antibacterial agents, *Archiv. Pharm. Res.* 35 (8) (2012) 1355–1368.
- [33] A.M. Hayallah, W.A. Elgaher, O.I. Salem, A.A. Alim, Design and synthesis of some new theophylline derivatives with bronchodilator and antibacterial activities, *Archiv. Pharm. Res.* 34 (1) (2011) 3–21.
- [34] Y. Voynikov, V. Valcheva, G. Momekov, P. Peikov, G. Stavrakov, Theophylline-7-acetic acid derivatives with amino acids as anti-tuberculosis agents, *Bioorg. Med. Chem. Lett.* 24 (14) (2014) 3043–3045.
- [35] World health statistics 2020: monitoring health for the SDGs, sustainable development goals. Geneva: World Health Organization; 2020. Licence: CC BY-NC-SA 3.0 IGO.
- [36] FDA's policy statement on the development of new stereoisomeric drugs (Stereomeric Drug Policy). *Fed. Regist.* 1992, 57: FR22249.
- [37] Committee for Proprietary Medical Products. Working Parties on Quality, Safety and Efficacy of Medicinal Products. Note for guidance: Investigation of chiral active substances (III/3501/91). Brussels: CPMP, 1993.

- [38] C. Brandel, Y. Amharar, J.M. Rollinger, U.J. Griesser, Y. Cartigny, S. Petit, G. Coquerel, Impact of molecular flexibility on double polymorphism, solid solutions and chiral discrimination during crystallization of diprophylline enantiomers, *Mol. Pharm.* 10 (10) (2013) 3850–3861.
- [39] L. Schjelderup, A.J. Aasen, F. Myhren, T. Pettersson, R. Kivekäs, One-pot Synthesis of (R)-(-)-Xanthinol Nicotinate, a Peripheral Vasodilator, Using (S)-(Chloromethyl)oxirane as Chiral Synthone, *Acta Chem. Scand.* 40b (1986) 505–507.
- [40] D. Grace, H. Hammer, A.J. Aasen, J.G.D. Daves, S.C.T. Svensson, B. Wigilius, Optical Resolution and Absolute Configuration of the Peripheral Vasodilator Xanthinol Nicotinate, *Acta Chem. Scand.* 39b (1985) 607–609.
- [41] M. Poterała, M. Dranka, P. Borowiecki, Chemoenzymatic Preparation of Enantiomerically Enriched (R)-(-)-Mandelic Acid Derivatives: Application in the Synthesis of the Active Agent Pemoline, *Eur. J. Org. Chem.* 2017 (16) (2017) 2290–2304.
- [42] P. Borowiecki, D. Paprocki, A. Dudzik, J. Plenkiewicz, Chemoenzymatic Synthesis of Proxiphylline Enantiomers, *J. Org. Chem.* 81 (2) (2016) 380–395.
- [43] P. Borowiecki, D. Paprocki, M. Dranka, First chemoenzymatic stereodivergent synthesis of both enantiomers of promethazine and ethopropazine, *Beilstein J. Org. Chem.* 10 (2014) 3038–3055.
- [44] G.V. Lima, M.R. da Silva, T. de Sousa Fonseca, L.B. de Lima, M.d.C.F. de Oliveira, T.L.G. de Lemos, D. Zampieri, J.C.S. dos Santos, N.S. Rios, L.R.B. Gonçalves, F. Molinari, M.C. de Mattos, Chemoenzymatic synthesis of (S)-Pindolol using lipases, *App. Catal. Gen.* 546 (2017) 7–14.
- [45] J. Albarrán-Velo, D. González-Martínez, V. Gotor-Fernández, Stereoselective biocatalysis: A mature technology for the asymmetric synthesis of pharmaceutical building blocks, *Biocatal. Biotrans.* 36 (2) (2017) 102–130.
- [46] A. Schülé, A. Merschaert, C. Szczepaniak, C. Maréchal, N. Carly, J. O'Rourke, C. Ates, A Biocatalytic Route to the Novel Antiepileptic Drug Brivaracetam, *Org. Proc. Res. Dev.* 20 (9) (2016) 1566–1575.
- [47] A.C. Carvalho, S. Fonseca Tde, M.C. de Mattos, C. de Oliveira Mda, T.L. de Lemos, F. Molinari, D. Romano, I. Serra, Recent Advances in Lipase-Mediated Preparation of Pharmaceuticals and Their Intermediates, *Int. J. Mol. Sci.* 16 (12) (2015) 29682–29716.

- [48] I.T. Lund, P.L. Bøckmann, E.E. Jacobsen, Highly enantioselective CALB-catalyzed kinetic resolution of building blocks for β -blocker atenolol, *Tetrahedron* 72 (46) (2016) 7288–7292.
- [49] M. Lopez-Iglesias, E. Busto, V. Gotor, V. Gotor-Fernandez, Chemoenzymatic asymmetric synthesis of 1,4-benzoxazine derivatives: application in the synthesis of a levofloxacin precursor, *J. Org. Chem.* 80 (8) (2015) 3815–3824.
- [50] P. Borowiecki, M. Bretner, Studies on the chemoenzymatic synthesis of (R)- and (S)-methyl 3-aryl-3-hydroxypropionates: the influence of toluene-pretreatment of lipase preparations on enantioselective transesterifications, *Tetrahedron Asymm.* 24 (15–16) (2013) 925–936.
- [51] C.A. Stewart, C.A. VanderWerf, Reaction of propylene oxide with hydrogen halides, *J. Am. Chem. Soc.* 76 (1954), 1259–1264.
- [52] P. Borowiecki, M. Dranka, A facile lipase-catalyzed KR approach toward enantiomerically enriched homopropargyl alcohols, *Bioorg. Chem.* 93 (2019) 102754.
- [53] P. Borowiecki, I. Justyniak, Z. Ochal, Lipase-catalyzed kinetic resolution approach toward enantiomerically enriched 1-(β -hydroxypropyl)indoles, *Tetrahedron Asymm.* 28 (12) (2017) 1717–1732.
- [54] P. Borowiecki, M. Dranka, Z. Ochal, Lipase-Catalyzed Kinetic Resolution of N-Substituted 1-(β -Hydroxypropyl)indoles by Enantioselective Acetylation, *Eur. J. Org. Chem.* 2017 (36) (2017) 5378–5390.
- [55] P. Borowiecki, S. Balter, I. Justyniak, Z. Ochal, First chemoenzymatic synthesis of (R)- and (S)-1-(9H-fluoren-9-yl)ethanol, *Tetrahedron Asymm.* 24 (18) (2013) 1120–1126.
- [56] P. Borowiecki, M. Fabisiak, Z. Ochal, Lipase-catalyzed kinetic resolution of 1-(1,3-benzothiazol-2-ylsulfanyl)propan-2-ol with antifungal activity: a comparative study of transesterification versus hydrolysis, *Tetrahedron* 69 (23) (2013) 4597–4602.
- [57] C.S. Chen, Y. Fujimoto, G. Girdaukas, C.J. Sih, Quantitative analyses of biochemical kinetic resolutions of enantiomers, *J. Am. Chem. Soc.* 104 (25) (1982) 7294–7299.
- [58] M. Meot-Ner, The ionic hydrogen bond, *Chem. Rev.* 105 (1) (2005) 213–284.
- [59] J.F. Beck, Y. Mo, How resonance assists hydrogen bonding interactions: an energy decomposition analysis, *J. Comp. Chem.* 28 (1) (2007) 455–466.
- [60] R.J. Kazlauskas, A.N.E. Weissfloch, A.T. Rappaport, L.A. Cuccia, A rule to predict which enantiomer of a secondary alcohol reacts faster in reactions catalyzed by cholesterol esterase, lipase from *Pseudomonas cepacia*, and lipase from *Candida rugosa*, *J. Org. Chem.* 56 (8) (1991) 2656–2665.

- [61] O. Trott, A.J. Olson, AutoDock Vina: improving the speed and accuracy of docking with a new scoring function, efficient optimization, and multithreading, *J. Comp. Chem.* 31 (2) (2010) 455–461.
- [62] J. Uppenberg, M.T. Hansen, S. Patkar, T.A. Jones, The sequence, crystal structure determination and refinement of two crystal forms of lipase B from *Candida antarctica*, *Structure* 2 (4) (1994) 293–308.
- [63] L. Brady, A.M. Brzozowski, Z.S. Derewenda, E. Dodson, G. Dodson, S. Tolley, J.P. Turkenburg, L. Christiansen, B. Huge-Jensen, L. Norskov, et al., A serine protease triad forms the catalytic centre of a triacylglycerol lipase, *Nature* 343 (6260) (1990) 767–770.
- [64] T.C. Bruice, F.C. Lightstone, Ground State and Transition State Contributions to the Rates of Intramolecular and Enzymatic Reactions, *Accounts of Chemical Research* 32(2) (1999) 127–136.
- [65] M. Cammenberg, K. Hult, S. Park, Molecular Basis for the Enhanced Lipase-Catalyzed N-Acylation of 1-Phenylethanamine with Methoxyacetate, *ChemBioChem* 7 (11) (2006) 1745–1749.
- [66] E.B. De Oliveira, C. Humeau, L. Chebil, E.R. Maia, F. Dehez, B. Maigret, M. Ghoul, J.-M. Engasser, A molecular modelling study to rationalize the regioselectivity in acylation of flavonoid glycosides catalyzed by *Candida antarctica* lipase B, *Journal of Molecular Catalysis B: Enzymatic* 59 (1–3) (2009) 96–105.
- [67] F. Ferrari, C. Paris, B. Maigret, C. Bidouil, S. Delaunay, C. Humeau, I. Chevalot, Molecular rules for chemo- and regio-selectivity of *Candida antarctica* lipase B in peptide acylation reactions, *J. Mol. Catal. B: Enzym.* 101 (2014) 122–132.
- [68] F. Hæffner, T. Norin, K. Hult, Molecular modeling of the enantioselectivity in lipase-catalyzed transesterification reactions, *Biophys. J.* 74 (3) (1998) 1251–1262.
- [69] T. Ema, J. Kobayashi, S. Maeno, T. Sakai, M. Utaka, Origin of the Enantioselectivity of Lipases Explained by a Stereo-Sensing Mechanism Operative at the Transition State, *Bull. Chem. Soc. Jp.* 71 (2) (1998) 443–453.
- [70] F. Hæffner, T. Norin, K. Hult, Molecular Modeling of the Enantioselectivity in Lipase-Catalyzed Transesterification Reactions, *Biophys. J.* 74 (3) (1998) 1251–1262.
- [71] I.J. Colton, D.T. Yin, P. Grochulski, R.J. Kazlauskas, Molecular Basis of Chiral Acid Recognition by *Candida rugosa* Lipase: X-Ray Structure of Transition State Analog and Modeling of the Hydrolysis of Methyl 2-Methoxy-2-phenylacetate, *Adv. Synth. & Catal.* 353 (13) (2011) 2529–2544.

- [72] G. Krasinski, M. Cypryk, M. Kwiatkowska, M. Mikołajczyk, P. Kielbasiński, Molecular modeling of the lipase-catalyzed hydrolysis of acetoxymethyl(*i*-propoxy)phenylphosphine oxide and its P-borane analogue, *J. Mol. Graph. Model.* 38 (2012) 290–297.
- [73] J.Y. Lim, N.Y. Jeon, A.R. Park, B. Min, B.T. Kim, S. Park, H. Lee, Experimental and Computation Studies on *Candida antarctica* Lipase B-Catalyzed Enantioselective Alcoholysis of 4-Bromomethyl- β -lactone Leading to Enantiopure 4-Bromo-3-hydroxybutanoate, *Adv. Synth. Catal.* 355 (9) (2013) 1808–1816.
- [74] A. Park, S. Kim, J. Park, S. Joe, B. Min, J. Oh, J. Song, S. Park, S. Park, H. Lee, Structural and Experimental Evidence for the Enantiomeric Recognition toward a Bulky *sec*-Alcohol by *Candida antarctica* Lipase B, *ACS Catal.* 6 (11) (2016) 7458–7465.
- [75] S. Raza, Enantioselectivity in *Candida antarctica* lipase B: A molecular dynamics study, *Protein Science* 10 (2) (2001) 329–338.
- [76] M. Topf, P. Varnai, W.G. Richards, Ab initio QM/MM dynamics simulation of the tetrahedral intermediate of serine proteases: insights into the active site hydrogen-bonding network, *J. Am. Chem. Soc.* 124 (49) (2002) 14780–14788.
- [77] S. Tomić, M. Ramek, Quantum mechanical study of *Burkholderia cepacia* lipase enantioselectivity, *J. Mol. Catal. B: Enzym.* 38 (3–6) (2006) 139–147.
- [78] A.M. Escorcía, M.C. Daza, M. Doerr, Computational study of the enantioselectivity of the O-acetylation of (R,S)-propranolol catalyzed by *Candida antarctica* lipase B, *Journal of Molecular Catalysis B: Enzymatic* 108 (2014) 21–31.
- [79] K. Świderek, S. Martí, V. Moliner, Theoretical Study of Primary Reaction of *Pseudozyma antarctica* Lipase B as the Starting Point To Understand Its Promiscuity, *ACS Catal.* 4 (2) (2014) 426–434.
- [78] P.B. Juhl, P. Trodler, S. Tyagi, J. Pleiss, Modelling substrate specificity and enantioselectivity for lipases and esterases by substrate-imprinted docking, *BMC Structural Biology* 9(1) (2009) 39.
- [79] M. Rodríguez-Mata, E. García-Urdiales, V. Gotor-Fernández, V. Gotor, Stereoselective Chemoenzymatic Preparation of β -Amino Esters: Molecular Modelling Considerations in Lipase-Mediated Processes and Application to the Synthesis of (S)-Dapoxetine, *Adv. Synth. Catal.* 352 (2–3) (2010) 395–406.
- [80] J. Yi, G. Du, Y. Yang, Y. Li, Y. Li, F. Guo, Chiral discrimination of natural isoflavanones using (R)- and (S)-BINOL as the NMR chiral solvating agents, *Tetrahedron Asymm.* 27 (22-23) (2016) 1153–1159.

- [81] P. Borowiecki, Enantiodifferentiation of promethazine using (S)-(-)-BINOL as the NMR chiral solvating agent: determination of the enantiomeric purity and performance comparison with traditional chiral HPLC, *Tetrahedron Asymm.* 26 (1) (2015) 16–23.
- [82] F. Yuste, R. Sánchez-Obregón, E. Díaz, M.A. García-Carrillo, Enantiodifferentiation of the antitumor alkaloid crispine A using the NMR chiral solvating agents (R)- and (S)-BINOL, *Tetrahedron Asymm.* 25 (3) (2014) 224–228.
- [83] J. Redondo, A. Capdevila, S. Ciudad, Determination of the enantiomeric purity of the antiasthmatic drug montelukast by means of ¹H NMR spectroscopy, *Chirality* 25 (11) (2013) 780–786.
- [84] J. Redondo, A. Capdevila, I. Latorre, Use of (S)-BINOL as NMR chiral solvating agent for the enantiodiscrimination of omeprazole and its analogs, *Chirality* 22 (5) (2010) 472–478.
- [85] K.D. Klika, M. Budovská, P. Kutschy, Enantiodifferentiation of phytoalexin spirobrassinin derivatives using the chiral solvating agent (R)-(+)-1,1'-bi-2-naphthol in conjunction with molecular modeling, *Tetrahedron Asymm.* 21 (6) (2010) 647–658.
- [86] J.S. Salsbury, P.K. Isbester, Quantitative ¹H NMR method for the routine spectroscopic determination of enantiomeric purity of active pharmaceutical ingredients fenfluramine, sertraline, and paroxetine, *Magn. Res. Chem.: MRC* 43 (11) (2005) 910–917.

Highlights

- The first successful enzyme-promoted synthesis of enantioenriched diprophylline and xanthinol nicotinate have been elaborated.
- The most potent biocatalytic system comprises of immobilized preparation of lipase B from *Candida antarctica* (Novozym 435) suspended in acetonitrile-methanol mixture.
- Molecular docking studies to predict enantiomers binding selectivity in CAL-B active site were performed.
- Single-crystal XRD analyses were performed for both the synthesized optically active APIs thus furnishing a first crystal structure of xanthinol nicotinate.

The authors declare that there is no conflict of interest.